Journal of the Mississippi Academy of Sciences

Volume 63 July/ October 2018 Numbers 3- 4

The Journal of the Mississippi Academy of Sciences (ISSN 0076-9436) is published in January (annual meeting abstracts), April, July, and October, by the Mississippi Academy of Sciences. Members of the Academy receive the journal as part of their regular (nonstudent) membership. Inquiries regarding subscriptions, availability of back issues, and address changes should be addressed to The Mississippi Academy of Sciences, Post Office Box 55709, Jackson, MS 39296-5709, telephone 601-977-0627, or email msacademyofscience@comcast.net.

Research Articles

Departments

STRAIN DIFFERENCES OF HEAT ADAPTED *Listeria monocytogenes* CELLS EXPOSED TO CARVACROL, ALKALI, H_2O_2 AND LAURIC ARGINATE (LAE)

Nitin Dhowlaghar, Mark W. Schilling and Ramakrishna Nannapaneni*

Department of Food Science, Nutrition and Health Promotion, Mississippi State University, Mississippi State, MS 39762, USA

Corresponding Author: Ramakrishna Nannapaneni, E-mail: nannapaneni@fsnhp.msstate.edu

ABSTRACT

The objective of the present study was to investigate the differences in survival of heat stressed *L. monocytogenes* strains ScottA, NRRL B- 33157 and F4260 in lethal levels of LAE (Lauric arginate), plant based essential oil (carvacrol) and disinfectants such as NaOH and H_2O_2 when incubated at both room temperature (22°C) and refrigeration temperature (4°C). The survival of all the three strains of heat stressed *L. monocytogenes* cells was higher by 1-2 logs in 33 ppm of LAE at room temperature as compared to the non-heat stressed cells. On the other hand, there was no change in the survival of heat stressed cells in 44 ppm of LAE at 4°C. The survival of all the three strains of heat stressed *L. monocytogenes* cells was higher by 1.5-2.5 log CFU/ml in 428 ppm of carvacrol at room temperature and 2.5-4.5 log CFU/ml in 535 ppm of carvacrol at 4°C. Strain differences were observed when exposed to lethal level of pH 12.5 NaOH. The heat stressed *L. monocytogenes* ScottA and NRRL B-33157 strains showed higher survival by 2.5 log CFU/ml at 22°C and did not show any change in the survival in pH 12.5 NaOH at 4°C. In addition, the heat stressed *L. monocytogenes* F4260 did not show any change in the survival in pH 12.5 NaOH at room temperature or 4°C. On the other hand, the survival of all the three strains of heat stressed *L. monocytogenes* cells decreased after exposure to 1000 ppm of H_2O_2 at room temperature and 1200 ppm of H_2O_2 at 4°C as compared to non-heat stressed cells. Therefore, this study indicate that the heat stressed cells of *L. monocytogenes* are not easily killed by LAE, carvacrol and alkali based antimicrobials.

Key words: *Listeria monocytogenes*, sublethal heat stress, cross protection, disinfectants, essential oils

INTRODUCTION

Listeria monocytogenes is a foodborne pathogen with ubiquitous nature and capable of surviving at diverse conditions including temperature range of 2-45°C, pH 3.5 – 12 and salt up to 10% which makes them highly prevalent in food processing areas (Farber and Peterkin 1991). *L. monocytogenes* is commonly isolated from meat products, dairy products, delicatessen products and seafood's and fruits and vegetables (Swaminathan and Gerner-Smidt 2007). *L. monocytogenes* causes listeriosis which is a deadly disease with a high mortality rate of 25-30% (Ramaswamy et al. 2007). Thirteen serotypes of *L. monocytogenes* are known, of which 1/2a, 1/2b, and 4b are responsible for most listeriosis outbreaks in the United States. Interestingly, *L. monocytogenes* serotype 1/2a is most often isolated from food but the majority of reported foodborne outbreaks have been caused by serotype 4b (Gandhi and Chikindas 2007).

Heating is one of the general practices carried out to control the growth of microorganisms in the food-processing plants and households. However, it was reported that pathogens might develop enhanced resistance to heat and other environmental stresses after exposure to sublethal heat which was known as heat tolerance response (Doyle et al. 2001; Skandamis et al. 2008). *L. monocytogenes* subjected to sublethal heat at 45°C for 60 min were more heat tolerant at 60°C compared to non-sublethally heated cells. In addition, a high diversity of heat tolerance within strains of *L. monocytogenes* serotypes were reported (Shen et al. 2014a). *L. monocytogenes* that undergone sublethal heat stress at 45°C for 10 min or 48°C for 60 min had higher resistance to other environmental stresses such as ethanol, chlorine and osmotic stresses. On the otherhand, sublethal heat stressed *L. monocytogenes* cells were not resistant to acid and QAC treatments (Doyle et al. 2001; Lin and Chou 2004; Lianou et al. 2006).

The use of essential oils (EOs) and lauric arginate (LAE) as antimicrobial agents in food processing industries are attracting much attention because they are considered as GRAS (generally recognized as safe) compounds (Burt 2004; Martin et al. 2009). However, it is likely that *L. monocytogenes* cells that encountered heat stress can induce cross-resistance to subsequent treatments with essential oils. One study demonstrated that *L. monocytogenes* heat shocked at 45°C for 1 h showed increased resistance to 200 ppm carvacrol (Ait-Ouazzou et al. 2013). The high stability of *L. monocytogenes* heat-stress adaptation after cooling step to 4°C could mainly result from the absence of active growth in such cold environment. Even though refrigeration temperature normally may delay the growth of *L. monocytogenes*, it may successfully preserve the acquired heat-stress adaptation resulting from the initial sublethal heat-stress treatment if occurred prior to cold storage (Pagán et al. 1997). However, there is limited data on the cross protection of *L. monocytogenes* sublethal heat stressed cells towards other environmental stresses at cold storage temperature.

The extensive diversity in nature of *L. monocytogenes* strains indicates that processing conditions cannot be standardized based on a particular standard strain alone. Hence, it is imperative to understand the characteristics of strain variation in *L. monocytogenes*. Therefore, in the present study the three *L. monocytogenes* strains that were categorized from low, medium and high heat tolerant groups were considered to study the survival of sublethal heat stress at 48°C for 1 h when exposed to carvacrol, H_2O_2, NaOH and Lauric arginate (LAE) stresses.

MATERIAL AND METHODS

Bacterial strains and growth conditions: Three *L. monocytogenes* strains that were categorized from our previous study as low, medium and high heat tolerant namely, ScottA, NRRL B-33157, and F4260 respectively belonged to 4b and 1/2a serotypes were used in this study. The strains was stored in -80°C in tryptic soy broth containing 0.6% yeast extract (TSBYE, pH 7.2; BD Bio sciences, San Jose, CA) supplemented with 16% glycerol. Working stock culture of this strain was maintained at 4°C in TSBYE. Ten ml of TSBYE was inoculated with a single colony of *L. monocytogenes* from the working stock culture, and incubated overnight in a shaker (C24 Classic series incubator shaker, New Brunswick Scientific, Inc., Edison, NJ, USA) at 37°C to reach stationary phase.

Induction of heat stress adaptation: To prepare the heat adapted cells of *L. monocytogenes*, one ml of stationary-phase culture was mixed with 10 ml of TSBYE that was pre-heated in to a reciprocal water bath shaker (model R76, New Brunswick Scientific, Inc., Edison, NJ, USA). The cells were then heated at 48 C for 60 min. After heat adaptation, the cell suspension was immediately used for studying the cross-protection studies. The non-adapted control cells were kept at room temperature for 1 h without exposure to sublethal stress.

Preparation of disinfectant solutions: The pH 12.0 lethal alkali treatment was prepared by adding 380 µl of 4M NaOH (Fisher Scientific, New Jersey, USA) to 10 ml of TSBYE. The lethal 1000 ppm of H_2O_2 (Acros Organics, New jersey, USA) was prepared by adding 800 µl of H_2O_2 (1.5%) to 10 ml of TSBYE. Carvacrol (>98%) was purchased from Sigma Aldrich (St. Louis, Mo., U.S.A.). It was solubilized by diluting (1:1) in propylene glycol (PG) (MP Biochemicals LLC, Solon, Ohio). The lethal concentration of carvacrol (428 ppm) was prepared by adding 70 µl of working stock concentration in TSBYE respectively. PG is a food additive approved by FDA with both solvent and emulsifying properties and *L. monocytogenes* is able to grow in concentrations up to 12.5% PG. The LAE solution obtained from Vedeqsa (Vedeqsa inc., New York, NY 10001) was approved by FDA at 200 ppm in food products (USFDA, 2005). The original solution (10%) of LAE was diluted by adding 100µl to 900µl in saline (0.85%) solution to obtain 1% LAE solution. Then for 33 and 41 ppm LAE solutions, 35 and 41µl of the prepared 1% solution was added to 9 ml TSB-YE broth respectively. Then 900µl of these LAE solutions were distributed in 1.5 ml eppendorf tubes for post-exposure treatments and allowed to be at either room temperature (RT) or 4°C depending upon the treatment temperatures. Carvacrol solution was purchased from Sigma Aldrich (St. Louis, Mo., U.S.A.). The concentrations of alkali and H_2O_2 were initially standardized for the controls (non-heated) cells and to compare the difference with the heat-stressed cells after post-exposure to alkali-stress or H_2O_2.

Survival of heat adapted and non-adapted *L. monocytogenes* cells to disinfectants and

antimicrobials: To perform the survival of heat stress adapted and non-adapted (control) *L. monocytogenes* cells in lethal disinfectants and antimicrobials, 1 ml of heat stressed or control cells were added to 9 ml of TSBYE containing disinfectants to yield 7 log CFU/ml. The post-exposure times of LAE and carvacrol were for 30 min each at room temperature or for up to 2 and 4 h, respectively, at 4°C. Survivors were enumerated by serial dilutions of the cell suspensions and by plating out on Tryptic soy agar containing yeast extract, esculin and ferric ammonium citrate (TSAYE-EF).

Statistical analysis: All experiments were performed in three replicates with three individual trials. Student *t*-test ($P < 0.05$) was performed using Microsoft excel to determine significant mean difference between survival of heat stress adapted and non-adapted control cells in lethal disinfectants or essential oils.

RESULTS

After sublethal heating at 48°C for 60 min, three strains of *L. monocytogenes* ScottA, NRRL B 33157 and F4260 showed greater survival ($P < 0.05$) by 1-2 log CFU/ml in 33 ppm of LAE exposure at room temperature (Figure. 1A, 1B and 1C). The sublethal heat-stressed and non-heated control cells of all three strains of *L. monocytogenes* did not show any significant difference at 4°C with 44 ppm LAE dose in this assay. After sublethal heating at 48°C for 60 min, three strains of *L. monocytogenes* ScottA, NRRL-B 33157 and F4260 showed greater survival ($P < 0.05$) by 1.5-2.5 log CFU/ml in 428 ppm of carvacrol exposure at room temperature and 2.5-4.5 log CFU/ml in 535 ppm of carvacrol at 4°C (Figure. 2A, 2B and 2C).

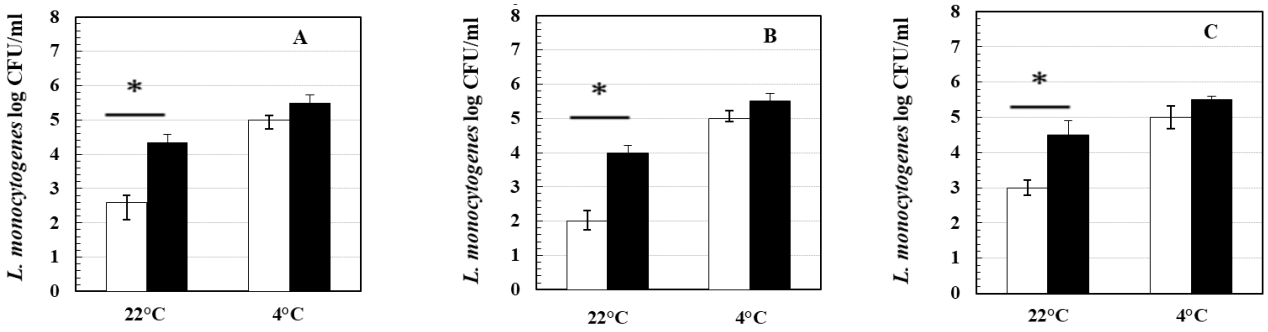

Figure 1: Effect of sublethal heat-stress at 48°C/30 min on survival in LAE treatment at room temperature (35 ppm/30 min) or 4°C (41ppm/2h) in three *L. monocytogenes* serotypes: (A) Bug600 (serotype 1/2a); (B) NRRL B-33157 (serotype 4b); and (C) F4260 (serotype 1/2b). No sublethal heating (□) or sublethal heating at 48°C (■). Sublethal heating treatments showing statistically higher survival are marked by asterisk ($P < 0.05$).

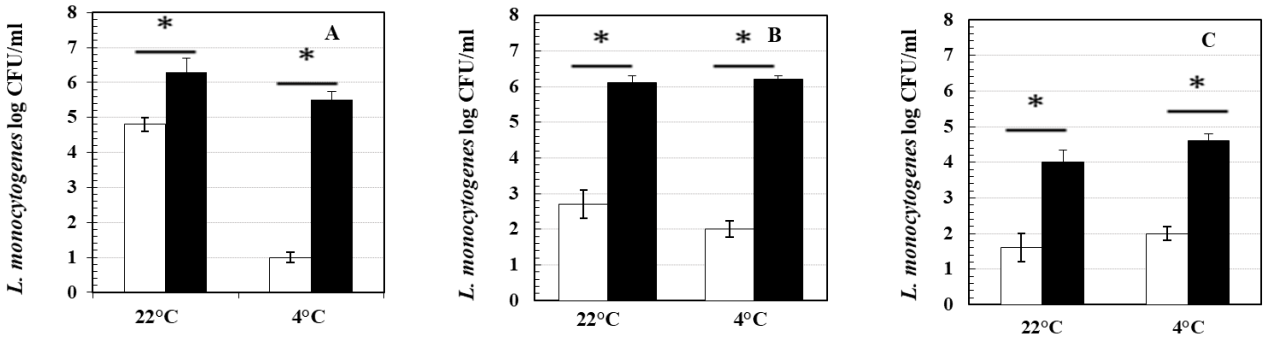

Figure 2: Effect of sublethal heat-stress at 48°C/30 min on survival in carvacrol treatment at room temperature (428 ppm/30 min) or 4°C (535ppm/4h) in three *L. monocytogenes* serotypes: (A) Bug600 (serotype 1/2a); (B)

NRRL B-33157 (serotype 4b; and (C) F4260 (serotype 1/2b). No sublethal heating (□) or sublethal heating at 48°C (■). Sub-lethal heating treatments showing statistically higher survival are marked by asterisk ($P < 0.05$).

Strain differences were observed when exposed to lethal alkali pH 12.5 NaOH. After sublethal heating at 48°C for 60 min, *L. monocytogenes* ScottA and NRRL B-33157 showed greater survival ($P < 0.05$) by approximately 2.5 log CFU/ml in pH 12.5 NaOH for 30 min at room temperature (Figure. 3A and B). On the other hand, *L. monocytogenes* F4260 did not show any difference in survival between sublethal heat stress and non-heat stressed cells (Figure 3C). In addition sublethal heat stressed *L. monocytogenes* ScottA cells showed greater survival ($P < 0.05$) by 1.5 log CFU/ml in pH 12.5 NaOH for 4 h at 4°C. Under the same conditions, other two strains NRRL B- 33157 and F4260 did not show any significant difference between sublethal heat stress and non-heat stressed cells. Similarly, after exposing to 1000 ppm of H_2O_2 for 30 min at room temperature and 1200 ppm of H_2O_2 for 4 h at 4°C, the sublethal heat stressed cells of all three *L. monocytogenes* strains were sensitive with approximately 2 log CFU/ml lesser survival ($P < 0.05$) as compared to non-heat stressed cells (Figure. 4A, 4B and 4C).

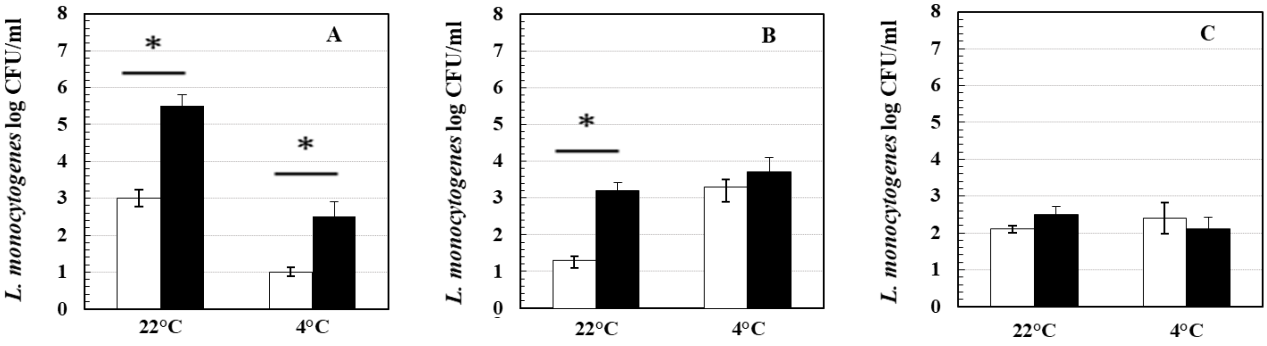

Figure 3: Effect of sublethal heat-stress at 48°C/30 min on survival in NaOH treatment at room temperature (12.5 pH/30 min) or 4°C (pH 12.5/4h) in three *L. monocytogenes* serotypes: (A) Bug600 (serotype 1/2a); (B) NRRL B-33157 (serotype 4b; and (C) F4260 (serotype 1/2b). No sublethal heating (□) or sublethal heating at 48°C (■). Sub-lethal heating treatments showing statistically higher survival are marked by asterisk ($P < 0.05$).

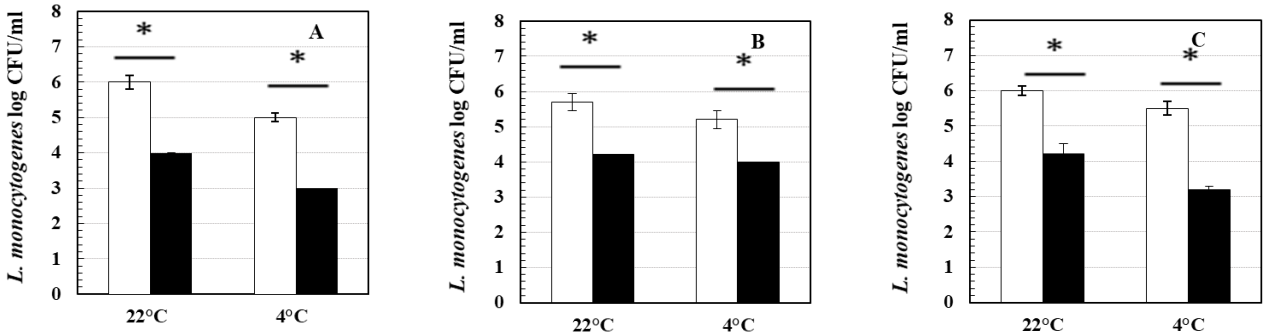

Figure 4: Effect of sublethal heat-stress at 48°C/30 min on survival in H_2O_2 treatment at room temperature (12.5 pH/30 min) or 4°C (pH 12.5/4h) in three *L. monocytogenes* serotypes: (A) Bug600 (serotype 1/2a); (B) NRRL B-33157 (serotype 4b; and (C) F4260 (serotype 1/2b). No sublethal heating (□) or sublethal heating at 48°C (■). Sub-lethal heating treatments showing statistically higher survival are marked by asterisk ($P < 0.05$).

DISCUSSION

In our previous studies, a significant increase in heat tolerance was observed after *L. monocytogenes* cells were exposed to sublethal heat stress at 48°C for 1 h (Shen et al. 2014b). In the present study, the cross-protection of *L. monocytogenes* sublethal heat stressed cells exposed to various disinfectants and essential oils at lethal levels was studied. Under room temperature, the limited lethal inactivation time was within 1 h as heat-stress adaptation was partially reversed within 1 h at room temperature depending on the strain. For those assays performed under 4°C, lethal inactivation time was not a limiting factor since up to 24 h *L. monocytogenes* cells were able to maintain acquired heat-stress adaptation. Since commonly used cleaners are either alkali- or oxidative-stress based, the survival responses of heat-stress adapted cells of *L. monocytogenes* in lethal concentration of alkali-stress and hydrogen peroxide were determined. Heat-stress adaptation conferred alkali-stress resistance appears to be strain dependent indicating the antimicrobial efficacy of alkali disinfectants could be undermined when heat-stress adapted cells are present. Similar observations were also reported by others which proposed that heat-stress adaptation in *L. monocytogenes* induces cross resistance to alkali based cleaners (Taormina and Beuchat 2001; Novak and Yuan 2003). For oxidative stress, a reverse pattern was observed that heat-stress adaptation rendered impaired survival in lethal concentration of hydrogen peroxide. H_2O_2 generates oxygen-free radicals that damages the cell membrane and disrupts the electron transport system. Present findings are in agreement with Lin and Chou, 2001, whereas Lou and Yousef observed increased survival in lethal H_2O_2. These distinct observations may be due to the differences in bacterial strains (Bug600 verses ScottA), physiological state of *L. monocytogenes* (stationary verses exponential phase) and heat adaptation conditions (45°C verses 48°C). Also, a reasonable explanation should be heat-stress adaptation caused down-regulation of oxidative related gene expression. However, so far no published data is available on how does heat-stress adaptation in *L. monocytogenes* modulates the oxidative stress related genes. Interestingly, in the presence of oxidative stress, survival of *L. monocytogenes* cells from low, medium and high groups exhibited the same order as their heat-stress resistance. According to our findings, oxidative chemical agents are more efficient in eliminating the heat-stress resistant phenotypes of *L. monocytogenes*. Heat-stress adapted cells survived slightly higher at room temperature as compared to 4°C in LAE treatment whereas enhanced carvacrol resistance in heat-stress adapted cells was evident at both temperatures tested. According to the literature, both compounds exhibit similar antimicrobial mechanism through interacting with the bacteria cell membrane (Kanazawa et al. 1995; Ultee et al. 2002). However, for control cells when the temperature was lowered from 22°C to 4°C it diminished antimicrobial efficacy of LAE while this type of efficacy reduction did not occur for carvacrol. Therefore, LAE and carvacrol might have different mode of action at 4°C which could be responsible for different cross resistance response of heat-stress adapted *L. monocytogenes* at 4°C.

CONCLUSIONS

The outcome of this study indicates that the heat stressed cells of *L. monocytogenes* are not easily killed by LAE, carvacrol and alkali based antimicrobials. These compounds should be carefully considered when different strains of sublethal heat stressed cells of *L. monocytogenes* may be present.

ACKNOWLEDGEMENT

This research was supported in part by Strategic Research Initiative and Food Safety Initiative awards to R. Nannapaneni from the Mississippi Agricultural and Forestry Experiment Station under project MIS-401160.

CONFLICT OF INTEREST

There is no conflict of interest to declare

LITERATURE CITED

1. Ait-Ouazzou, A., Espina, L., Gelaw, T., Lamo-Castellví, S., Pagán, R. and García-Gonzalo, D. (2013). "New insights in mechanisms of bacterial inactivation by carvacrol". *Journal of Applied microbiology* **114**, 173-185.
2. Burt, S. (2004). "Essential oils: their antibacterial properties and potential applications in foods—a review". *International journal of food microbiology* **94**, 223-253.
3. Doyle, M.E., Mazzotta, A.S., Wang, T., Wiseman, D.W. and Scott, V.N. (2001). "Heat resistance of

Listeria monocytogenes." Journal of Food Protection® **64**, 410-429.

4. Farber, J. and Peterkin, P. (1991). "*Listeria monocytogenes*, a food-borne pathogen." *Microbiological reviews* **55**, 476-511.
5. Gandhi, M. and Chikindas, M.L. (2007). "*Listeria*: a foodborne pathogen that knows how to survive." *International journal of food microbiology* **113**, 1-15.
6. Kanazawa, A., Ikeda, T. and Endo, T. (1995). "A novel approach to mode of action of cationic biocides: morphological effect on antibacterial activity." *The Journal of applied bacteriology* **78**, 55-60.
7. Lianou, A., Stopforth, J.D., Yoon, Y., Wiedmann, M. and Sofos, J.N. (2006). "Growth and stress resistance variation in culture broth among *Listeria monocytogenes* strains of various serotypes and origins." *Journal of Food Protection*® **69**, 2640-2647.
8. Lin, Y.-D. and Chou, C.-C. (2004). "Effect of heat shock on thermal tolerance and susceptibility of *Listeria monocytogenes* to other environmental stresses." *Food microbiology* **21**, 605-610.
9. Martin, E., Griffis, C., Vaughn, K., O'Bryan, C., Friedly, E., Marcy, J., Ricke, S., Crandall, P. and Lary Jr, R. (2009). "Control of *Listeria monocytogenes* by lauric arginate on frankfurters formulated with or without lactate/diacetate." *Journal of food science* **74**.
10. Novak, J.S. and Yuan, J.T. (2003). "Viability of Clostridium perfringens, Escherichia coli, and *Listeria monocytogenes* surviving mild heat or aqueous ozone treatment on beef followed by heat, alkali, or salt stress." *Journal of Food Protection*® **66**, 382-389.
11. Pagán, R., Condón, S. and Sala, F. (1997). "Effects of several factors on the heat-shock-induced thermotolerance of *Listeria monocytogenes*." *Applied and environmental microbiology* **63**, 3225-3232.
12. Ramaswamy, V., Cresence, V.M., Rejitha, J.S., Lekshmi, M.U., Dharsana, K., Prasad, S.P. and Vijila, H.M. (2007)."*Listeria*-review of epidemiology and pathogenesis." *Journal of Microbiology Immunology and Infection* **40**, 4.
13. Shen, Q., Jangam, P.M., Soni, K.A., Nannapaneni, R., Schilling, W. and Silva, J.L. (2014a). "Low, medium, and high heat tolerant strains of *Listeria monocytogenes* and increased heat stress resistance after exposure to sublethal heat." *Journal of Food Protection*® **77**, 1298-1307.
14. Shen, Q., Jangam, P.M., Soni, K.A., Nannapaneni, R., Schilling, W. and Silva, J.L. (2014b). "Low, medium, and high heat tolerant strains of *Listeria monocytogenes* and increased heat stress resistance after exposure to sublethal heat." *J Food Prot* **77**, 1298-1307.
15. Skandamis, P.N., Yoon, Y., Stopforth, J.D., Kendall, P.A. and Sofos, J.N. (2008). "Heat and acid tolerance of *Listeria monocytogenes* after exposure to single and multiple sublethal stresses." *Food microbiology* **25**, 294-303.
16. Swaminathan, B. and Gerner-Smidt, P. (2007)."The epidemiology of human listeriosis." *Microbes and Infection* **9**, 1236-1243.
17. Taormina, P.J. and Beuchat, L.R. (2001). "Survival and heat resistance of *Listeria monocytogenes* after exposure to alkali and chlorine." *Appl Environ Microbiol* **67**, 2555-2563.
18. Ultee, A., Bennik, M. and Moezelaar, R. (2002). "The phenolic hydroxyl group of carvacrol is essential for action against the food-borne pathogen *Bacillus cereus*." *Applied and environmental microbiology* **68**, 1561-1568.

A Tripodal Thiourea Receptor for Naked-Eye Detection of Sulfate via Fluoride Displacement Assay

Corey R. Johnson,[1] Mohammad H. Hasan,[2] Maryam Emami Khansari,[1] Ritesh Tandon[2] and Md. Alamgir Hossain*[1]

[1]Department of Chemistry and Biochemistry, Jackson State University, Jackson, MS 39217
[2]Department of Microbiology and Immunology, University of Mississippi Medical Center, Jackson, MS 39216

Corresponding Author: Alamgir Hossain Email: alamgir.hossain@jsums.edu

ABSTRACT

A thiourea-based tripodal receptor substituted with 3-nitrophenyl groups has been studied for the binding of anions by ^{1}H NMR and UV-Vis titrations in DMSO-d_6. The receptor has been shown to bind an anion, showing the strong selectivity for sulfate. A competitive colorimetric assay in the presence of fluoride suggests that the bound fluoride can be displaced by sulfate, exhibiting a visible color change. The receptor was further tested for its biocompatibility on and HeLa cells, demonstrating an excellent cell viability up to 100 µM concentration.

Keywords:

INTRODUCTION

Anions play an important role in many environmental and biological systems, and the mechanistic understanding of selective anion recognition by synthetic receptors is critical in the field of supramolecular chemistry (Bowman-James and Bianchi, 2012). Although polyamine-based receptors are known to bind anions strongly, their binding occurs only at a certain pH, hampering their practical application under neutral conditions (Hossain, 2008). On the other hand, neutral receptors including amides, ureas, and thioureas are suitable for binding anions with their H-bond donor groups regardless of the solution pH (Bondy, 2003; Amendola *et al*, 2010; Bose *et al*, 2012). Recently, tren-based receptors bearing urea, or thiourea functional groups have been an area of focus for anion recognition, due to the directional conformation and enhanced chelation effect of the NH groups (Custelcean *et al*, 2005). The electron withdrawing nature of sulfur on thiourea functionalities increases the acidity of NH for H-bonding interactions with an anionic guest (Khansari *et al*, 2017). Furthermore, attaching chromophore groups to receptors often leads to a spectroscopic or color change, allowing them to serve as sensors for target analytes (Gale *et al*, 2016; Gale *et al,* 2017). Herein, we report a thiourea-based tripodal receptor **L**, Furthermore, attaching chromophore groups to receptors often leads to a spectroscopic or color change, allowing them to serve as sensors for target analytes (Gale *et al*, 2016; Gale *et al,* 2017). Herein, we report a thiourea-based tripodal receptor **L (Figure 1)**, showing strong selectivity for sulfate. The selectivity was further supported by competitive colorimetric studies, displaying a sharp visible color change upon the addition of sulfate to the fluoride complex of **L**.

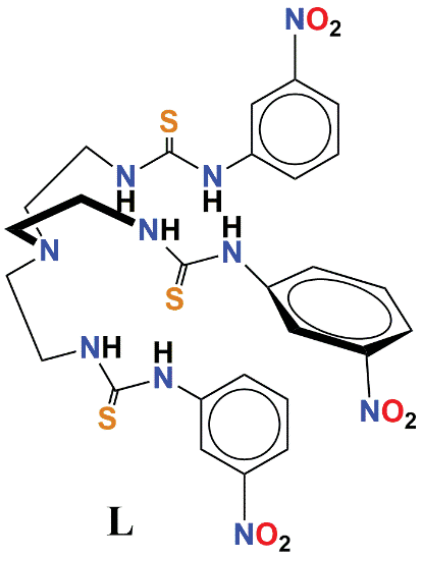

Figure 1. Receptor **L**.

METHODS

General: All reagents and solvents were purchased as reagent grade and were used without further purification. Nuclear magnetic resonance (NMR) spectra were recorded on a Varian Unity INOVA 500 FT-NMR. Chemical shifts for samples were measured in DMSO-d_6 and calibrated against sodium salt of 3-(trimethylsilyl) propionic-2,2,3,3-d_4 acid (TSP) as an external reference in a sealed capillary tube. NMR data were processed and analyzed with MestReNova Version 6.1.1-6384. The IR spectra were recorded on a Perkin Elmer-Spectrum One FT-IR spectrometer with KBr disks in the range of 4000–400 cm^{-1}. The melting point was determined on a Mel-Temp (Electrothermal 120 VAC 50/60 Hz) melting point apparatus and was uncorrected. Mass spectral data were obtained at ESI-MS positive mode on a TSQ Quantum GC (Thermo Scientific). Elemental analysis was carried out using an ECS 4010 Analytical Platform (Costech Instrument) at Jackson State University.

Synthesis: The receptor L was synthesized following the literature procedure (Khansari *et al*, 2017).

NMR Binding Studies: Binding constants were obtained by ^{1}H NMR titrations of L with the oxoanions (NO_3^-, ClO_4^-, $H_2PO_4^-$, HSO_4^-, and SO_4^{2-}) and halides (F^-, Cl^-, Br^-, and I^-) using their tetrabutyl ammonium salts in DMSO-d_6. Initial concentrations were $[L]_0 = 2$ mM, and $[anion]_0 = 20$ mM. Each titration was performed by 13 measurements at room temperature. The association constant K was calculated by fitting of several independent NMR signals with a 1:1 association model (Schneider *et al,* 1998).

UV-Vis Binding Studies: UV-Vis titration studies were performed by titrating L with anions in DMSO at 25 ºC. In this case, initial concentrations of L and the anions were 1.5 x 10^{-4} M and 1.5 x 10^{-2} M, respectively. Each titration was performed by 15 measurements ($[A^-]_0/[L]_0 = 0$–35 equivalents), and the binding constant K was calculated by fitting the relative UV-Vis absorbance (I/I_0) with a 1:1 association model (Schneider *et al,* 1998).

Cytotoxicity Assay: Primary human foreskin-derived fibroblasts (HF) and HeLa cells were grown in Dulbecco's modified Eagle's medium (DMEM) (Cellgro, Manassas, VA) supplemented with 10% fetal bovine serum (SAFC, Lenexa, KS), 1 mM sodium pyruvate, 2 mM L-glutamine, 4.5 g/ml glucose, and 100 U/ml penicillin-streptomycin (Cellgro) at 37°C with 5% CO_2 (Freshney, 2005). Cells were seeded in 12-well plates and grown until they became confluent (approximately 24 hours). The media was removed, and fresh complete medium was added. A stock solution of L was made in 100% DMSO at 500 mM concentration. Cells were treated with L at a final concertation of 10 µM to 500 µM in different wells for 24 hours for cytotoxic assessment. In this experiment, 0.1% was the highest concentration of DMSO that the cells received. As a mock control, cells were treated with 0.1 % DMSO without L. At the end point, cells were observed under an inverted Evos-FL microscope (Thermo Fisher Scientific, Waltham, MA), and bright-field images of living cells were captured. After imaging, the viability of cells was determined using trypan blue exclusion assay as previously described (Strober, 2001; Archer *et al*, 2017; Freshney 2005).

RESULTS

NMR titration studies: ^{1}H NMR titrations of L were performed to evaluate its binding affinity for a variety of anions (F^-, Cl^-, Br^-, I^-, ClO_4^-, NO_3^-, $H_2PO_4^-$, HSO_4^-, and SO_4^{2-}) using their tetrabutylammonium salts in DMSO-d_6. Figure 1 shows the stacking of ^{1}H NMR spectra as obtained from the titration of L with SO_4^{2-} (0-10 eq.). In the ^{1}H NMR spectrum of L, one NH proton is observed at 10.01 (H1) ppm and the other one at 7.95 (H2) ppm. The addition of SO_4^{2-} to L resulted in a significant downfield shift of both NH signals ($\Delta\delta$= 1.49 ppm for H1 and $\Delta\delta$= 1.81 ppm for H2) with a sharp saturation at a 1:1 ratio (Figure 2), demonstrating strong interactions of the receptor and sulfate. Similar downfield shifts in the NH signals, but to a lesser extent, were also observed for HSO_4^- ($\Delta\delta$= 0.72 ppm for H1 and $\Delta\delta$= 0.71 ppm for H2), Cl^- ($\Delta\delta$= 0.61 ppm for H1 and $\Delta\delta$= 0.38 ppm for H2) and Br^- ($\Delta\delta$= 0.09 ppm for H1 and $\Delta\delta$= 0.06 ppm for H2) at the end of titrations. The NH signals of L were shown to be broadened and eventually disappeared upon the addition of $H_2PO_4^-$. In this case, CH signals were used to calculate the binding constant. However, for I^-, NO_3^- and ClO_4^-, a negligible change in the NMR signals was observed. The binding constants of L for these anions were determined from a nonlinear

regression analysis of the progressive changes of NH or CH signals with a 1:1 binding model (Schneider *et al*, 1988). The binding data are listed in Table 1, showing that the receptor binds strongly to SO_4^{2-}, with an association constant larger than 10^4 M^{-1} (Table 1).

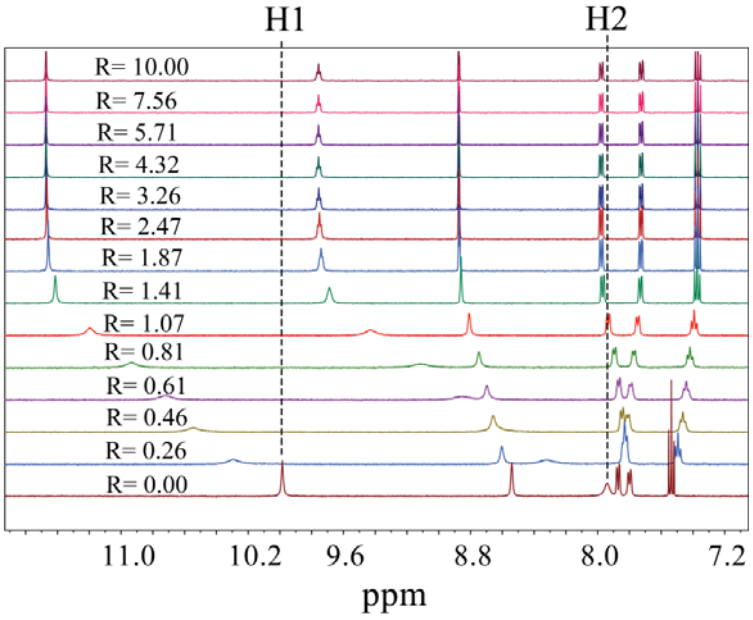

Figure 2. Partial ^{1}H NMR spectra of L (2 mM) showing changes in the NH chemical shifts with an increasing amount of SO_4^{2-} (20mM) in DMSO-d_6. (H1 = CSN*H*Ar and H2 = CH_2N*H*CS).

Table 1. Binding constants (log *K*) and binding energies (*E*) of the anions complexes of L.

Anion	Log K^a	Log K^b
F^-	> 4.0 [c]	5.1
Cl^-	3.1	3.2
Br^-	1.9	1.7
I^-	<1 [d]	<1 [e]
SO_4^{2-}	> 4.0	6.4
HSO_4^-	2.9	2.8
$H_2PO_4^-$	3.0	3.1
NO_3^-	<1 [d]	<1 [e]
ClO_4^-	<1 [d]	<1 [e]

[a] Determined by ^{1}H NMR titrations in DMSO-d_6; [b] determined by UV titrations in DMSO; [c] slow proton exchange; [d] no appreciable change was observed in ^{1}H NMR spectra; [e] no appreciable change was observed in UV spectra.

In contrast, upon the addition of fluoride to L, a new set of NMR signals appeared at downfield via a slow proton exchange between the free receptor and the complex. The signals of the free receptor disappeared completely upon the addition of one equivalent of fluoride (Figure 3). There is some evidence that highly basic anions can abstract acidic protons from NH of urea/thiourea-based compounds (Boiocchi *et al*, 2005). A detailed study on deprotonation and hydrogen bonding aspects between anions and urea/thiourea-based receptors reported by Pérez-Casas and Yatsimirsky (2008) suggested that the deprotonation is accompanied by the disappearance of NMR signals of the abstracted protons, while the binding event results in the downfield shift of NMR signals of NH groups in a receptor. The distinct downfield shift of NH signals in our receptor is consistent with the formation of a hydrogen-bonded complex (instead of deprotonation). For further clarification, a control experiment was carried out using OH^-, showing complete disappearance of NH signals due to the deprotonation of NH by highly basic hydroxide ions (E, Figure 3).

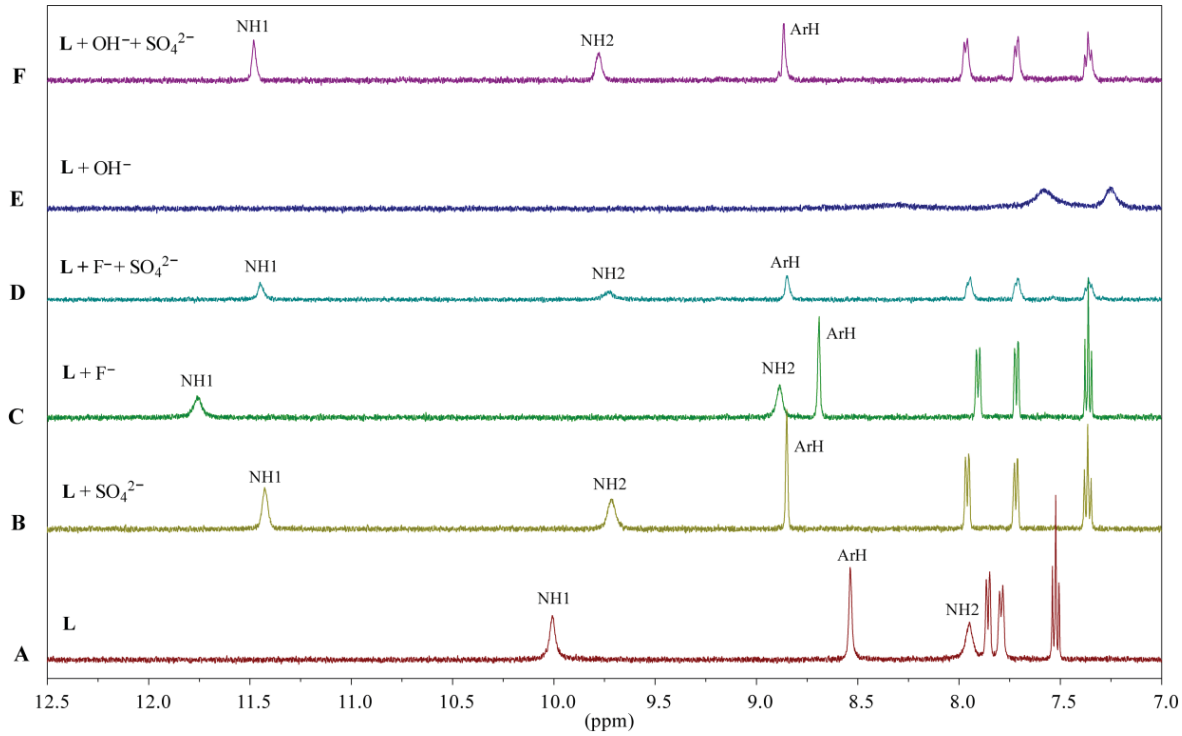

Figure 3. Partial ^{1}H NMR spectra of L showing changes in the chemical shifts after the addition of one equivalent of different anions in DMSO-d_6.

The binding constant for fluoride was calculated from the relative changes in the integrated intensity of NH signals for the free receptor and the complex, yielding a binding constant larger than 10^4 M^{-1} (Portis *et al*, 2017). To determine the selectivity of the receptor, competition experiments were performed in which sulfate was added to the receptor containing one equivalent of fluoride (C, Figure 3) or hydroxide (E, Figure 3) in DMSO-d_6. As shown in Figure 3, the ^{1}H NMR spectrum of L containing an equivalent amount of fluoride and sulfate (D), or hydroxide and sulfate (F), resembles the spectrum of L containing one equivalent of sulfate (B), thus demonstrating the selectivity of the receptor for sulfate. The receptor also exhibits good interactions for Cl^-, HSO_4^-, and $H_2PO_4^-$ with association constants of 3.1, 2.9 and 3.0 (in log *K*), respectively. However, it does not show any appreciable affinity for I^-, NO_3^-, or ClO_4^-.

Colorimetric studies: The receptor was further investigated by naked eye colorimetric studies for anions in DMSO. As shown in Figure 4, a visible color change from pale yellow to orange was observed after the addition of one equivalent of fluoride to L (2 mM), indicating a different optical absorption spectrum of the $[LF]^-$ complex. However, the color remained almost unchanged for other anions. A similar color change was reported previously due to the addition of fluoride to related receptors (Khansari *et al*, 2014). To examine the visual selectivity, one equivalent of different anions was added separately to an orange solution of fluoride complex in DMSO. Interestingly, the color of $[LF]^-$ was sharply changed to a pale yellow color (original color of the receptor) after the addition of sulfate. This observation suggests that sulfate can compete with fluoride for hydrogen bonding with NH groups, and displace the bound fluoride from the complex $[LF]^-$ into solution, which agrees with NMR competition experiments (Figure 5). However, other anions are not strong enough to displace the bound fluoride, supporting the results of NMR and UV-Vis titrations. Thus, the fluoride-receptor complex serves as a colorimetric probe for visual identification of sulfate through *fluoride displacement assay*, a principle that is known as an *indicator displacement assay* widely used for optical sensing of analytes (Nguyen and Anslyn, 2006; Rhaman *et al*, 2014).

Figure 4. Colorimetric studies of the receptor L (2 mM) with one equivalent of different anions in DMSO.

Figure 5. Colorimetric studies of $[LF]^-$ after the addition of one equivalent of different anions in DMSO, showing a visual color change for sulfate.

UV-Vis titration studies: UV-Vis titrations were also performed to investigate the interactions of the receptor with anions in DMSO. As shown in Figure 6, the addition of sulfate to a solution of L results in a systematic decrease in the absorbance with a red shift of the peak at 335 nm, suggesting the formation of a $[L(SO_4)]^{2-}$ complex. The relative absorbance I/I_0 of L (where I_0 and I represent the absorbance of L before and after the addition of an anion, respectively) upon the gradual addition of SO_4^{2-} gave the best fit to a 1:1 binding mode yielding a binding constant of 6.40 (in log *K*). The host showed a similar spectral change when it was titrated with dihydrogen phosphate. The addition of fluoride anion to L also showed a decrease in the absorption at 335 nm, but no appreciable shift was observed as compared to that for sulfate or phosphate. However, the naked-eye colorimetric study shows an orange color after the addition of just one equivalent of fluoride to the receptor in which the concentration of L was different (2 mM) than that used in UV titrations (0.15 mM).

To confirm if the color originated from the binding with fluoride (instead of deprotonation), the receptor was deprotonated by adding one equivalent of hydroxide. The resulting intense red color of the deprotonated receptor is distinctly different than that developed for the fluoride complex, suggesting that the observed orange color (for the receptor containing fluoride) originated from the binding event (Figure 7). Further justification of this assumption is provided by control experiments from UV studies of the receptor containing one equivalent of hydroxide or fluoride in DMSO (Figure 8). In the UV spectrum, a new absorption band appeared at about 485 nm for the solution of L containing hydroxide anion, indicating an anion-induced deprotonation of L due to the removal of NH protons by highly basic OH^-. However, such a band is absent for the solution of L containing fluoride. The addition of one equivalent sulfate to L mixed with fluoride (or hydroxide) shows a nearly similar spectrum to that obtained from the sulfate complex. This further supports the displacement of the bound fluoride by sulfate, which is in accordance with the NMR results discussed previously. On the other hand, the addition of other anions to L solution does not induce an appreciable change in the absorption spectrum. This observation is fully consistent with colorimetric observations, showing no visible color change for Cl^-, Br^-, I^-, ClO_4^-, NO_3^-, and HSO_4^-.

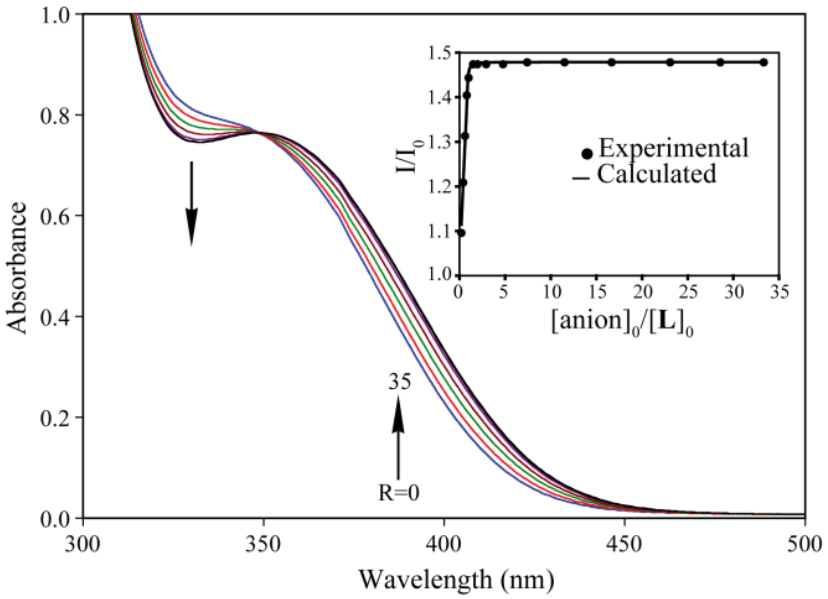

Figure 6. UV-Vis titration spectra showing the changes in absorption spectra of L (1.5×10^{-4} M) with an increasing amount of SO_4^{2-} (1.5×10^{-2} M) in DMSO (Inset showing the titration plot).

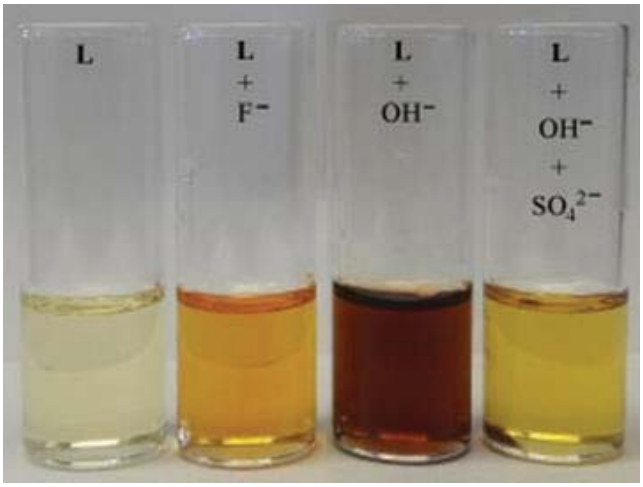

Figure 7. Colorimetric studies of L (2 mM) after the addition of one equivalent of fluoride, hydroxide or a mixture of fluoride and hydroxide in DMSO, showing different color.

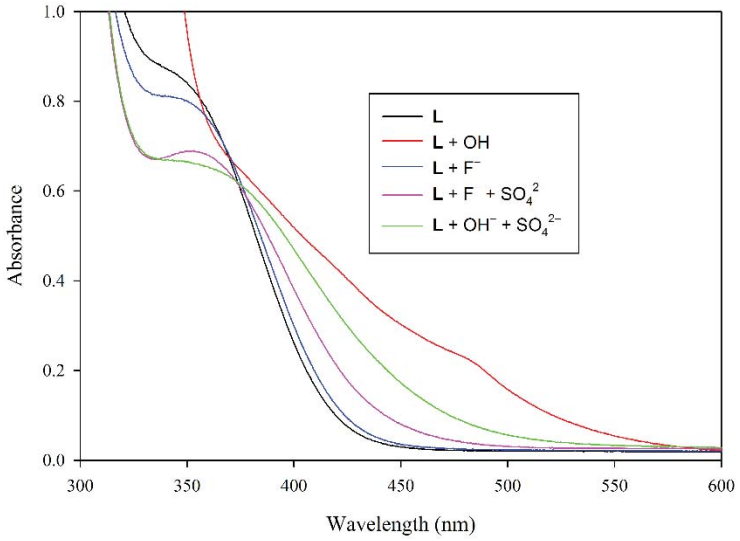

Figure 8. UV-vis spectra of L (1.5 x 10^{-4} M) with 5 equivalents of different anions in DMSO.

Cytotoxicity Assessment: The biocompatibility of L as a receptor was tested by analyzing the viability on HeLa cells. Each type of cells was treated with L at concentrations ranging from 10 µM to 500 µM for 24 hours, and the cell viability was quantified using a trypan blue exclusion assay. As a control, cells were treated with 0.1% DMSO. The results from the exclusion assay revealed that the cell viability of HeLa cells was almost unaffected up to 100 µM concentration of the receptor (Figure 9). However, the cell cytotoxicity was observed at a higher concentration (500 µM). Live cell imaging was also performed on HeLa cells at 24 hours post treatment, showing no cytotoxic effects upto 100 µM (Figure 10). These results are in accord with the cell viability data, further demonstrating an excellent biocompatibility of the receptor on living cells.

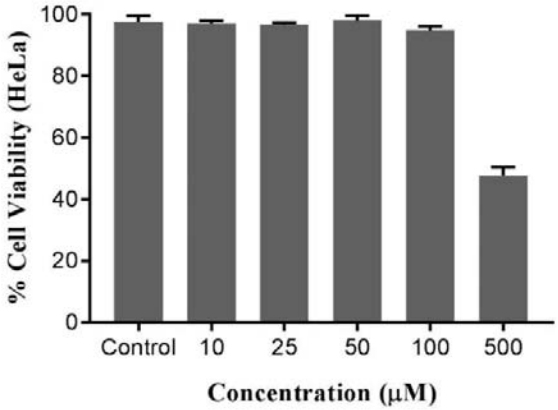

Figure 9. Effect of L on cell viability. Confluent HeLa cells were either mock treated (0.1 % DMSO-treated control) or treated with L (10 μM to 500 μM) for 24 hours. Triplicate samples were used, and error bars represent standard error of mean.

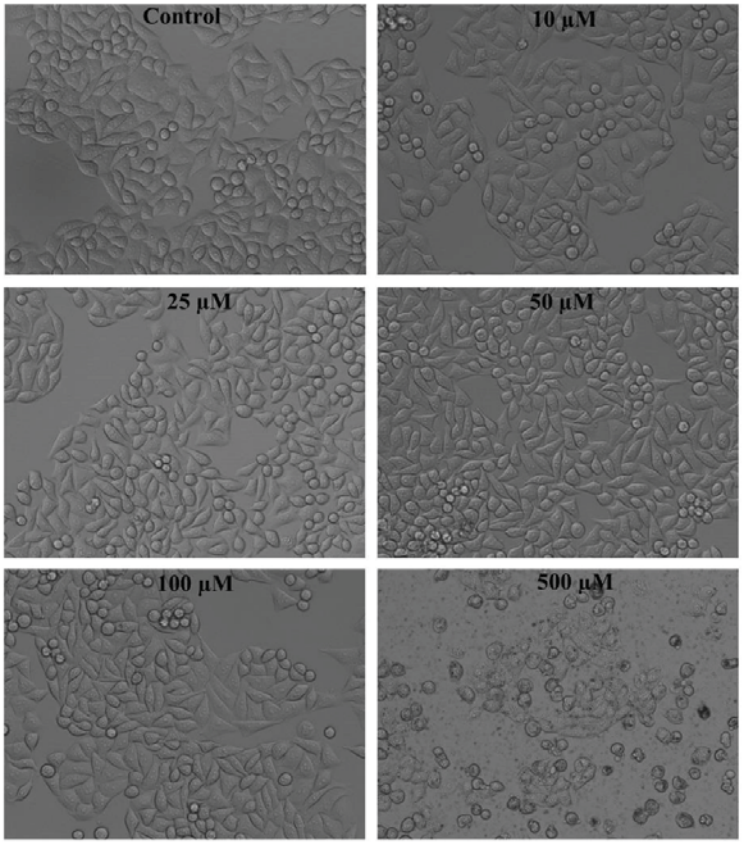

Figure 10. Bright-field images of HeLa cells. Cells were either mock treated (0.1% DMSO-treated control) or treated with L for 24 hours at the concentrations specified. Images are representative of three independent experiments.

CONCLUSIONS

In conclusion, we have synthesized and structurally characterized a thiourea-based tripodal receptor L, showing strong binding and selectivity for sulfate over other anions in DMSO. The selectivity of L for sulfate was further confirmed by the competitive colorimetric studies, displaying a sharp color change of $[LF]^-$, while other anions showed no change in color. This observation suggests that the added sulfate displaces the bound fluoride in $[LF]^-$, and this compound can be used as a colorimetric probe to detect sulfate in solution *via* a fluoride displacement assay. The strong selectivity of L for sulfate was further supported by UV-Vis titrations in DMSO. The receptor also shows an excellent biocompatibility in HeLa cells. The strong selectivity for sulfate and excellent biocompatibility towards living cells demonstrates that this receptor can be used as a potential sensing probe for the detection of sulfate anions for various biological and chemical applications.

ACKNOWLEDGMENTS

The National Science Foundation is acknowledged for a CAREER award (CHE-1056927) to M.A.H. NMR core facility at Jackson State University was supported by the National Institutes of Health (G12RR013459). M.H.H. and R.T. are supported by American Heart Association (Award No. 14SDG20390009).

LITERATURE CITED

Amendola, V.; Fabbrizzi, L.; Mosca, L. Anion recognition by hydrogen bonding: urea-based receptors. *Chem. Soc. Rev*. **2010**, *39*, 3889–3915.

Archer, M. A.; Brechtel, T. M.; Davis, L. E.; Parmar, R. C.; Hasan, M. H.; Tandon, R. Inhibition of endocytic pathways impacts cytomegalovirus maturation. *Sci. Rep.* **2017**, *7*, 46069.

Boiocchi, M., Del Boca, L., Esteban-Gómez, D., Fabbrizzi, L., Licchelli, M. and Monzani, E. Anion-induced urea deprotonation. *Chem. Eur. J*. **2005**, *11*, 3097–3104.

Bondy, C. R.; Loeb, S. J. Amide based receptors for anions. *Coord. Chem. Rev*. **2003**, *240*, 77–99.

Bose, P.; Dutta, R.; Santra, S.; Chowdhury, B.; Ghosh, P. Combined solution-phase, solid-phase and phase-interface anion binding and extraction studies by a simple tripodal thiourea receptor. *Eur. J. Inorg. Chem*. **2012**, *35*, 5791–5801.

Bowman-James, K., Bianchi, A., Garcia-España, E. Anion Coordination Chemistry. Wiley-VCH. New York. 2012.

Custelcean, R.; Moyer, B. A.; Hay, B. P. A coordinatively saturated sulfate encapsulated in a metal-organic framework functionalized with urea hydrogen-bonding groups. *Chem. Commun*. **2005**, *48*, 5971–5973.

Freshney, R. I. Culture of animal cells. Eds. John Wiley & Sons. New York. 2005.

Gale, P. A.; Howe, E. N. W.; Wu, X. Anion receptor chemistry. *Chem.* **2016**, *1*, 351–422.

Hossain, M. A. Inclusion complexes of halide anions with macrocyclic receptors. *Curr. Org. Chem*. **2008**, *12*, 1231–1256.

Khansari, M. E.; Wallace, K. D.; Hossain, M. A. Synthesis and anion recognition studies of a dipodal thiourea-based sensor for anions. *Tetrahedron Lett*. **2014**, *55*, 438–440.

Khansari, M. E.; Hasan, M. H.; Johnson, C. R; Williams, N. A.; Wong, B. M.; Powell, D. R.; Tandon, R.; Hossain, M. A. Anion Complexation Studies of 3-Nitrophenyl-Substituted Tripodal Thiourea Receptor: A Naked-Eye Detection of Sulfate via Fluoride Displacement Assay. *ACS Omega.* **2017**, *(*DOI: 10.1021/acsomega.7b01485).

Nguyen, B. T.; Anslyn, E. V. Indicator–displacement assays. *Coord. Chem. Rev.* **2006**, *250*, 3118–3127.

Pérez-Casas, C. Yatsimirsky, A. K. Detailing hydrogen bonding and deprotonation equilibria between anions and urea/thiourea derivatives. *J. Org. Chem.* **2008**, *73*, 2275-2284.

Portis, B.; Mirchi, A.; Emami Khansari, M.; Pramanik, A.; Johnson, C. R.; Powell, D. R.; Leszczynski, J.; Hossain, M. A. An ideal C_3-symmetric sulfate complex: molecular recognition of oxoanions by *m*-nitrophenyl- and pentafluorophenyl-functionalized hexaurea receptors. *ACS Omega*. **2017**, *2*, 5840-5849.

Rhaman, M. M.; Alamgir, A.; Wong, B. M.; Powell, D. R.; Hossain,M. A. A highly efficient dinuclear Cu(II) chemosensor for colorimetric

and fluorescent detection of cyanide in water. *RSC Advances* **2014**, *4*, 54263–54267.

Schneider, H. J.; Kramer, R.; Simova, S.; Schneider, U. Solvent and salt effects on binding constants of organic substrates in macrocyclic host compounds. A general equation measuring hydrophobic binding contributions. *J. Am. Chem. Soc.* **1988**, *110*, 6442–6448.

Strober, W., Trypan blue exclusion test of cell viability. *Curr. Protoc. Immunol*. **2001**. *Appendix 3*, Appendix 3B.

DIFFERENCES IN SURVIVAL OF HEAT STRESS ADAPTED CELLS OF *Listeria monocytogenes* EGD (BUG 600) IN DISINFECTANTS AND ESSENTIAL OILS

Nitin Dhowlaghar[1], Qian Shen[1], Piumi De. A. Abeysundara[1], Amruta Udaysinh Jadhav, Ramakrishna Nannapaneni[1]*, Mark W. Schilling, Wen-Hsing Cheng, and Chander S. Sharma[2]

[1]Department of Food Science, Nutrition and Health Promotion, Mississippi State University, Mississippi State, MS 39762, USA and [2]Poultry Science Department, Mississippi State University, Mississippi State, MS 39762, USA.

Corresponding Author: Ramakrishna Nannapaneni, E-mail: nannapaneni@fsnhp.msstate.edu

ABSTRACT

Listeria monocytogenes exhibits increased heat tolerance to lethal heating temperature when pre-exposed to sublethal heat stress. The objective of this study was to investigate the differences in survival of *L. monocytogenes* EGD (Bug600) (serotype 1/2a) in various disinfectants and essential oils after sublethal heat stress at 48°C for 60 min. The survival of heat stressed *L. monocytogenes* cells was lower in lethal acid (HCl or H_3PO_4 pH 2.5), lethal oxidative stress (H_2O_2 1000 ppm) and lethal quaternary ammonium compounds (QAC 2.5-3.5 ppm) than the non-stressed control cells. By contrast, the survival of heat stressed *L. monocytogenes* cells was higher when exposed to lethal alkali (NaOH or KOH pH 12) than the control. In essential oils, the survival of heat stressed *L. monocytogenes* cells was higher when exposed to lethal carvacrol (428 ppm) and bay oil (1100 ppm) and the survival was lower in red thyme oil (300 pm) compared to control. On the other hand, there was no change in the survival of heat stressed cells in lethal cinnamon oil (1050 ppm) compared to control. This study indicated that the heat stressed cells of *L. monocytogenes* are not easily killed by NaOH- or KOH-based alkaline disinfectants, and in essential oils containing carvacrol and bay oil. Therefore, these sanitizers should be carefully considered when sublethal heat stressed cells of *L. monocytogenes* may be present.

Keywords: *Listeria monocytogenes*, heat stress adaptation, cross protection, disinfectants, essential oils

INTRODUCTION

Listeria monocytogenes is a Gram-positive, facultative anaerobic foodborne pathogen associated with a variety of food products such as meat, poultry, fresh produce and dairy products (Farber and Brown, 1990; Gandhi and Chikindas, 2007). *L. monocytogenes* was also isolated from various environment settings such as soil, ground water and decaying vegetation (Gray et al., 2006). Ingestion of *L. monocytogenes* via contaminated foods leads to listeriosis, a severe disease that primarily affects immunocompromised individuals, pregnant women, senior individuals and newborns. The fatality rate of listeriosis ranges from 20 to 30 % (Hamon et al., 2006). *L. monocytogenes* has a potential to persist for extended periods of time under mild processing environments such as heat, acid and alkaline conditions (Vasseur et al., 1999). Exposure to these mild sublethal conditions subsequently induces stress tolerance response in which these initial mild stress shocks provide edge to *L. monocytogenes* cells in subsequent survival under lethal stress conditions (Ramaswamy et al., 2007; Yousef and Courtney, 2003). There are several reports indicating that exposure to particular mild stress can also lead to enhanced protection against other lethal stress which was defined as cross protection (Soni et al., 2011).

Heating is the most reliable end point preservation technique used in food industries for inactivation of microbes. *L. monocytogenes* heat stress adaptation is defined as pre-exposing cells at a sublethal heat stress which confers increased heat tolerance at lethal heating temperature (Farber and Brown, 1990). This increased thermal tolerance is partially due to the activation of conserved heat shock proteins (Hsps) (e.g., DnaK and GroEL) under sublethal heat temperatures (Doyle et al., 2001; Ferreira et al., 2001; Hill et al., 2002).

Chemical disinfectants such as chlorine, quaternary ammonium compounds (QACs) and alkali containing compounds are frequently applied in cleaning and sanitation to inactivate undesirable microorganisms. In the food processing environment, contaminated *L. monocytogenes* may encounter sublethal heat stress that activates its intracellular stress responses and become persistent in the subsequent lethal inactivation by these disinfectants (Taormina and Beuchat, 2001). Studies show that *L. monocytogenes* cells heat shocked at 45°C for 1 h had increased tolerance to 25% NaCl, 18% ethanol and 0.01% crystal violet (Lin and Chou, 2004). Lin et al. (2012) observed that *L. monocytogenes* cells heat stressed at 48°C for 10 min were more tolerant to 0.128 ppm of chlorine dioxide and 1.384 ppm of QACs compared to non-adapted control cells (Lin et al., 2012). The viability of heat stressed cells of *L. monocytogenes* in other disinfectant is not known.

Plant essential oils (EOs) are gaining interest for their potential use as antimicrobials in the food industries as they are recognized as generally recognized as safe (GRAS). Many studies show that EOs can efficiently kill pathogenic *Escherichia coli*, *Salmonella* Spp. and *L. monocytogenes* in standard microbiology growth media or in various food substrates (Burt, 2004; Skandamis and Nychas, 2001; Smith-Palmer et al., 2001). It is likely that if the initial treatments which fail to kill the *L. monocytogenes* cells can provide them with cross protection against EOs. One study demonstrated that *L. monocytogenes* heat shocked at 45°C for 1 h showed increased resistance to 200 ppm carvacrol (Ait‐Ouazzou et al., 2013). There is no information on the sensitivity of heat stressed *L. monocytogenes* cells to other EOs. Therefore, the objective of this study was to determine the effect of heat stress adaptation on the survival of *L. monocytogenes* Bug600 in various disinfectants and essential oils.

MATERIALS AND METHODS

Bacterial strains and growth conditions: L. monocytogenes EGD (Bug600, serotype 1/2a (Institut Pasteur, Paris, France) was used in this study. The strain was stored in -80°C in tryptic soy broth containing 0.6% yeast extract (TSBYE, pH 7.2; BD Bio sciences, San Jose, CA) supplemented with 16% glycerol. Working stock culture of this strain was maintained at 4°C in TSBYE. Ten ml of TSBYE was inoculated with a single colony of L. monocytogenes from the working stock culture, and incubated overnight in a shaker (C24 Classic series incubator shaker, New Brunswick Scientific, Inc., Edison, NJ, USA) at 37°C to reach stationary phase.

Induction of heat stress adaptation: The sublethal heat stress adaptation was performed by adding 1 ml of stationary-phase culture to 9 ml of TSBYE and heating at 48°C for 1 h. A reciprocal water bath shaker (model R76, New Brunswick Scientific, Inc., Edison, NJ, USA) was used for heating. Inoculum was directly added into the pre-heated broth and mixed so that the inoculum did not adhere to non-heated part of inner tube wall and cap. The non-adapted control cells were kept at room temperature for 1 h without exposure to sublethal stress.

Preparation of disinfectant solutions: Disinfectants used in this study was shown in Table 1. The working stock concentrations for H_3PO_4 (5,625 ppm), QAC-1 (187 ppm), QAC-2 (525 ppm) and CPC (400 ppm) were prepared by diluting the original stock solution by 1:100 in deionized water. The working stock concentration of H_2O_2 (15,000 ppm) was prepared by diluting 428 µl of the original stock solution in 10 ml deionized water. Carvacrol (>98%), Bay oil (100%), Red thyme oil (100%) and cinnamon leaf oil (>99%) were purchased from Sigma Aldrich (St. Louis, Mo., U.S.A.). These essential oils were solubilized by diluting (1:1) in propylene glycol (PG) (MP Biochemicals LLC, Solon, Ohio) and required concentrations were then prepared in TSBYE as described in Table 2. PG is a food additive approved by FDA with both solvent and emulsifying properties and L. monocytogenes is able to grow in concentrations up to 12.5% PG.

Exposure of heat adapted and non-adapted L. monocytogenes cells to disinfectants and essential oils: To determine the survival of heat stress adapted and non-adapted (control) L. monocytogenes Bug600 cells in lethal disinfectants and essential oils, 1 ml of heat stressed or control cells were added to 9 ml of TSBYE containing disinfectants at 22°C to yield an initial cell concentration of 7 log CFU/ml. Except for the QACs and NaOH, incubation time for all the disinfectants and essential oils was 60 min and survivors were enumerated every 15 min by plating on Tryptic soy agar containing yeast extract, esculin and ferric ammonium citrate (TSAYE-EF). Cells were exposed to QACs for 30 min and to NaOH for 120 min and survivors were enumerated every 10 min or 30 min on TSAYE-EF.

Statistical analysis: All experiments were performed in three replicates with three individual trials. Student t-test ($P < 0.05$) was performed using Microsoft excel to determine significant mean difference between survival of heat stress adapted and non-adapted control cells in lethal disinfectants or essential oils.

Table 1. Preparation of disinfectants.

Disinfectant group	Active ingredient	Manufacturers	Concentration of active ingredient (ppm)	Lethal concentration tested
Acid	HCl	Fisher Scientific	330,000	pH 2.5
	H_3PO_4	Sigma Aldrich	224,000	pH 12.0
Alkaline	NaOH	Fisher Scientific	160,000	pH 12.0
	KOH	Diversey	5,625	pH 2.5
Oxidative	NaOCl	The Clorox company	60,000	800 ppm
	H_2O_2	Acros Organics	350,000	1200 ppm
Quaternary ammonium compounds	QAC-1[1]	Lysol	18,700	3.5 ppm
	QAC-1[2]	Diversey	52,500	3.5 ppm
	CPC[3]	Safe foods corporation	4,000	2.5 ppm

[1]QAC-1 (Lysol) contains dimethylbenzyl ammonium chloride (C_{14} 60%, C_{16} 30%, C_{12} 5%, C_{18} 5%)

[2]QAC-2 (D-trol) contains dimethylbenzyl ammonium chloride (C_{14} 60%, C_{16} 30%, C_{12} 5%, C_{18} 5%) and dimethylbenzyl ammonium chloride (C_{12} 68%, C_{14} 32%)

[3]Cetylpyridinium chloride (Cecure) contains 1-Hexadecylpyridinium chloride

Table 2. Preparation of essential oils.

Essential oils	Active Ingredients	Manufacturers	Working stock conc. (ppm)	Lethal conc. tested (ppm)
Carvacrol	5-isopropyl-2-methylphenol	Sigma Aldrich	61,250	428
Bay oil	a-pinene, b-pinene, myrcene, limonene, linalool, methyl chavicol, neral, a-terpineol, geranyl acetate, eugenol and chavicol	Sigma Aldrich	62,500	1100
Red thyme oil	[a]N/A	Sigma Aldrich	62,500	300
Cinnamon leaf oil	[a]N/A	Sigma Aldrich	61,875	1050

[a]N/A represents that the composition of the essential oil is unknown.

RESULTS

The survival of heat stress adapted cells of L. monocytogenes Bug600 in lethal HCl and H_3PO_4 is shown in Fig. 1. The heat stress adapted L. monocytogenes cells were sensitive to lethal HCl and H_3PO_4 compared to non-adapted control cells. The survival of heat stress adapted cells was significantly decreased by 2 log CFU/ml in pH 2.5 by HCl after 60 min compared to control cells ($P < 0.05$) (Fig. 1A). Similarly, in the presence of pH 2.5 by H_3PO_4, the heat stress adapted cells were non-detectable after 60 min while control cells had a survival of 4.7 log CFU/ml under those conditions ($P < 0.05$) (Fig. 1B).

The survival of heat stress adapted cells of *L. monocytogenes* Bug600 in lethal NaOH and KOH is shown in Fig. 2. The heat stress adapted *L. monocytogenes* cells had significantly higher survival in lethal NaOH and KOH compared to control cells. The survival of heat stress adapted *L. monocytogenes* cells was significantly increased by 4.3 and 2.2 log CFU/ml in lethal NaOH and KOH (pH 12) respectively ($P < 0.05$) (Fig. 2A and B) after 120 min compared to control cells which were non-detectable under those conditions.

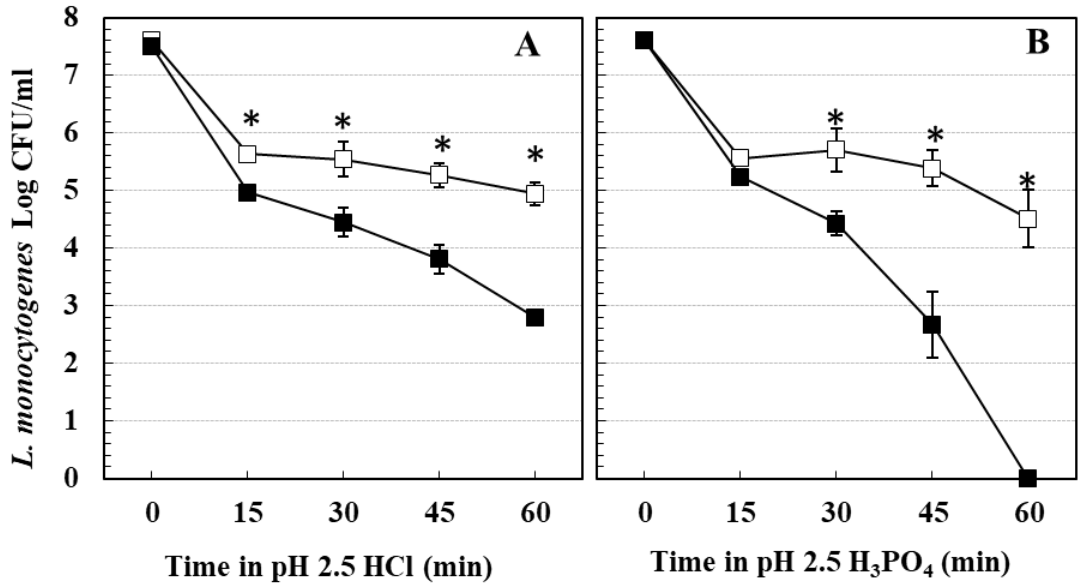

Figure 1. Survival of *L. monocytogenes* Bug600 in pH 2.5 HCl (A) and pH 2.5 H_3PO_4 (B) at 22ºC after 1 h pre-exposure to 48°C (■) or no sublethal heating (□). Symbols marked with an asterisk indicate significant survival differences between heat adapted (■) and non-adapted (□) cells.

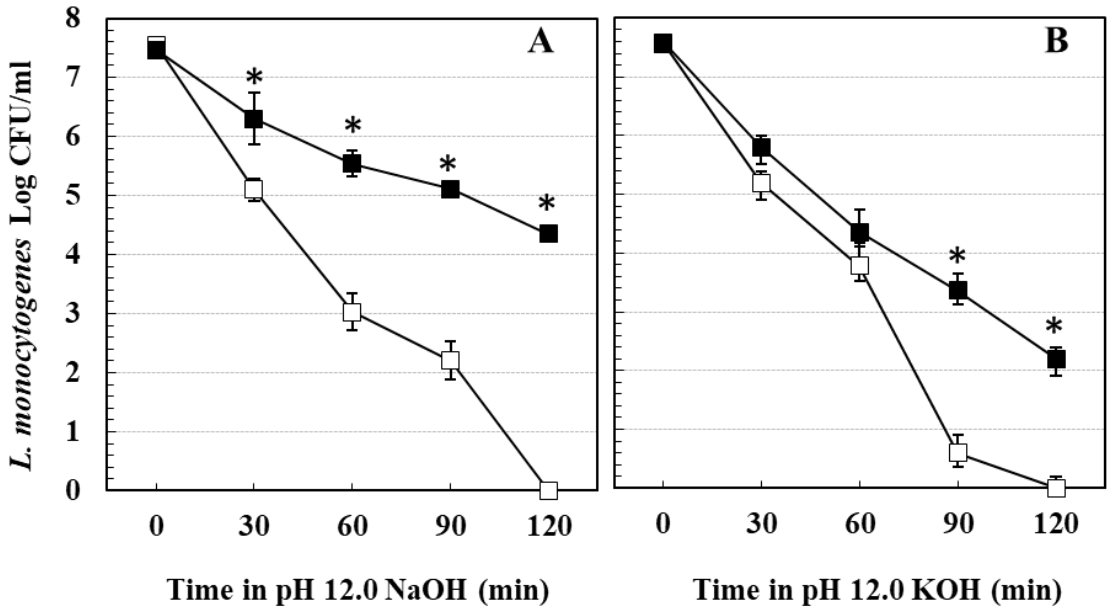

Figure 2. Survival of *L. monocytogenes* Bug600 in pH 12.0 NaOH (A) and pH 12.0 KOH (B) at 22ºC after 1 h pre-exposure to 48°C (■) or no sublethal heating (□). Symbols marked with an asterisk indicate significant survival differences between heat adapted (■) and non-adapted (□) cells.

The survival of heat stress adapted cells of *L. monocytogenes* Bug600 in lethal Lysol, D-trol and CPC is shown in Fig. 3-4. The heat stress adapted *L. monocytogenes* cells were sensitive to Lysol, D-trol and CPC compared to non-adapted control cells. The survival of heat stress adapted cells were significantly decreased by about 3.0 log CFU/ml in Lysol or D-trol (3.5 ppm) after 30 min compared to control cells ($P < 0.05$). Also, the survival of heat stress adapted cells was significantly decreased by 4.4 log CFU/ml in 2.5 ppm CPC compared to control cells which were non-detectable at 60 min ($P < 0.05$) (Fig. 4).

The survival of heat stress adapted cells of *L. monocytogenes* Bug600 in lethal NaOCl and H_2O_2 is shown in Fig. 5. The heat stress adapted *L. monocytogenes* cells were sensitive to NaOCl and H_2O_2 compared to non-adapted control cells. The survival of heat stress adapted cells was significantly decreased by 3.0 log CFU/ml in lethal NaOCl (800 ppm) after 60 min compared to control cells ($P < 0.05$) (Fig. 5A). Also, the survival heat stress adapted cells was significantly decreased by 2.0 log CFU/ml in lethal H_2O_2 (1200 ppm) compared to control cells ($P < 0.05$) (Fig. 5B).

The survival of heat stress adapted cells of *L. monocytogenes* Bug600 in lethal essential oils is shown in Fig. 6. *L. monocytogenes* heat stress adapted cells had significantly increased in survival in lethal carvacrol and bay essential oils compared to non-adapted control cells (Fig. 6A and B). The survival of heat stress adapted cells was significantly increased by 2.5 log CFU/ml in lethal carvacrol (428 ppm) (Fig. 6A) or by 3.5 log CFU/ml in lethal bay oil (1100 ppm) (Fig. 6B) compared to control cells ($P < 0.05$). By contract, the heat stress adapted *L. monocytogenes* cells were sensitive to red thyme oil (300 ppm) where the survival of *L. monocytogenes* was significantly decreased by 1.4 log CFU/ml compared to control cells ($P < 0.05$) (Fig. 6C). On the other hand, there was no significant difference in survival of *L. monocytogenes* heat stress adapted and non-adapted control cells in lethal cinnamon oil (1050 ppm) (Fig. 6D).

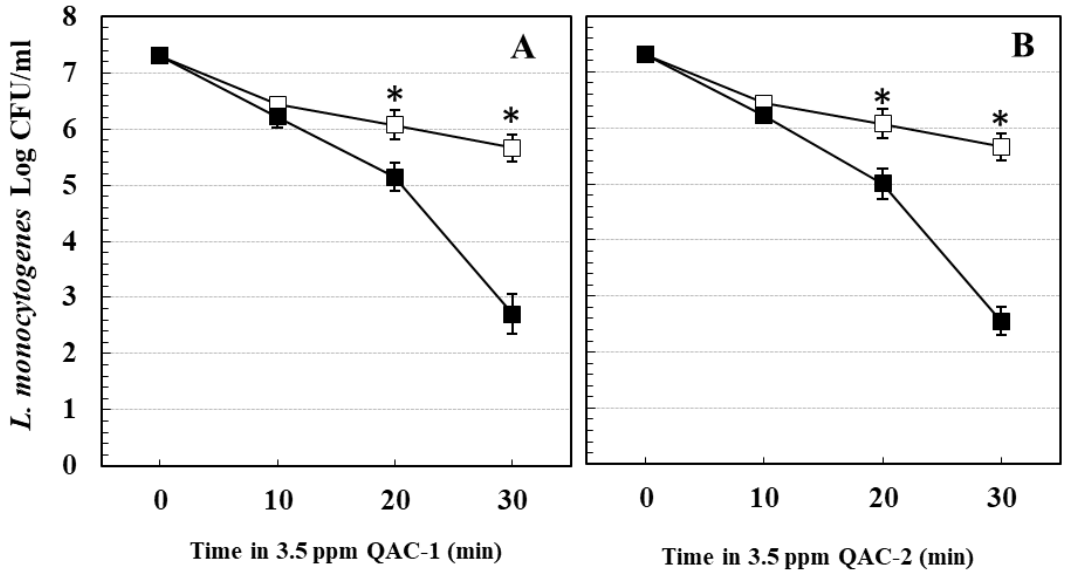

Figure 3. Survival of *L. monocytogenes* Bug600 in 3.5 ppm QAC-1 (A) and 3.5 ppm QAC-2 (B) at 22ºC after 1 h pre-exposure to 48°C (■) or no sublethal heating (□). Symbols marked with an asterisk indicate significant survival differences between heat adapted (■) and non-adapted (□) cells.

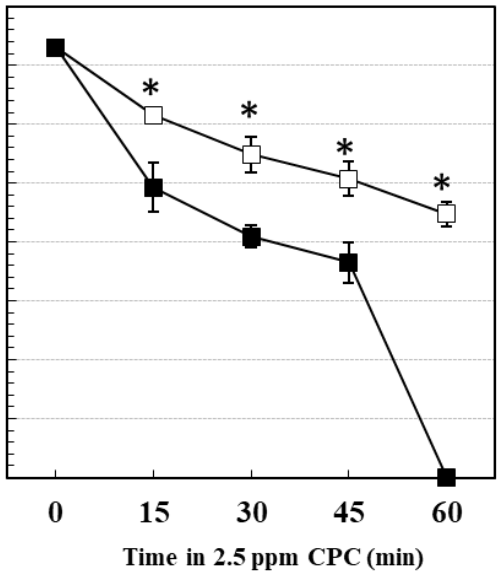

Figure 4. Survival of *L. monocytogenes* Bug600 in 2.5 ppm CPC at 22ºC after 1 h pre-exposure to 48°C (■) or no sublethal heating (□). Symbols marked with an asterisk indicate significant survival differences between heat adapted (■) and non-adapted (□) cells.

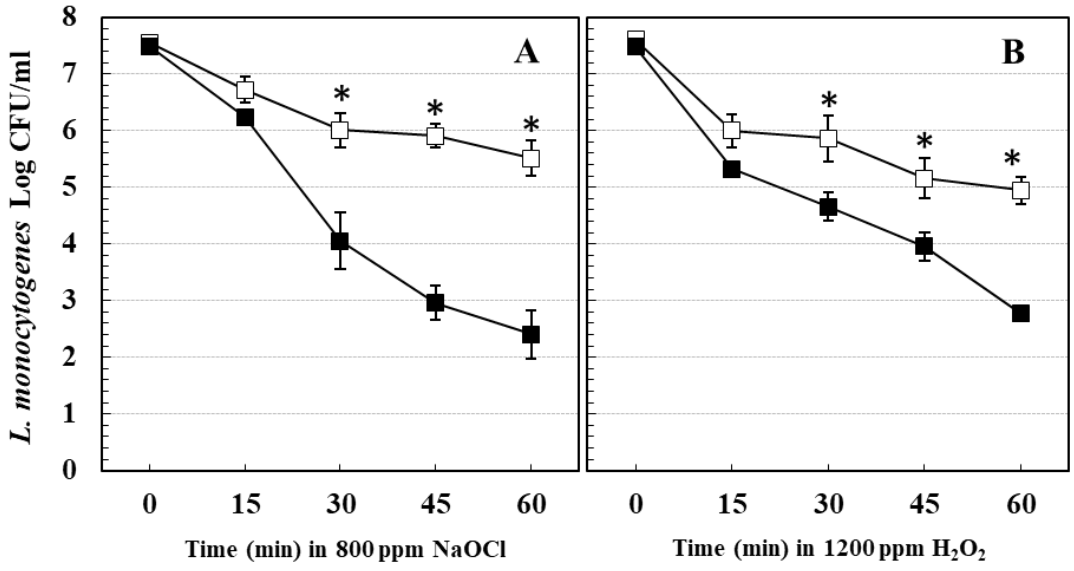

Figure 5. Survival of *L. monocytogenes* Bug600 in 800 ppm NaOCl (A) and 1200 ppm H_2O_2 (B) at 22ºC after 1 h pre-exposure to 48°C (■) or no sublethal heating (□). Symbols marked with an asterisk indicate significant survival differences between heat adapted (■) and non-adapted (□) cells.

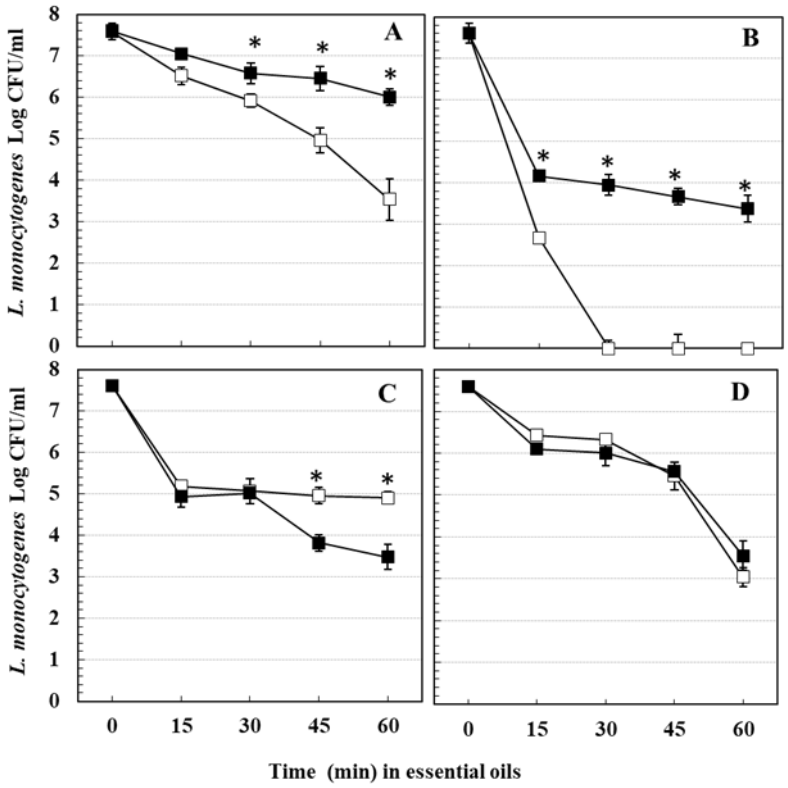

Figure 6. Survival of *L. monocytogenes* Bug600 in 428 ppm Carvacrol (A), 1100 ppm Bay oil (B), 300 ppm Red thyme (C) and 1050 ppm Cinnamon (D) at 22ºC after 1 h pre-exposure to 48°C (■) or no sublethal heating (□). Symbols marked with an asterisk indicate significant survival differences between heat adapted (■) and non-adapted (□) cells.

DISCUSSION

Despite the routine use of antimicrobials and disinfectants, *L. monocytogenes* may still persist in some food processing environments due to its tolerance to various antimicrobial compounds (Davidson and Harrison, 2002). Heating is a reliable end point preservation technique followed in food industries for inactivation of foodborne pathogens. However, heat stress adaptation due to insufficient heat inactivation may allow *L. monocytogenes* cells to survive during the second round of heat inactivation or in mild heat treatments (e.g., microwave) prior to consumption (Doyle et al., 2001).

Our findings show that the heat stress adapted *L. monocytogenes* Bug600 cells were more sensitive to lethal acid stress by HCl and H_3PO_4 compared to control cells. Similar phenomenon has been reported by Lou and Yousef (Lou and Yousef, 1997) and Lee et al.(Lee et al., 1995) in *L. monocytogenes* and *S.* Typhimurium where heat adapted cells were more sensitive to lethal acidic pH than non-adapted control cells. Although no molecular mechanisms have been elucidated on how heat adaptation in *L. monocytogenes* resulted in increased sensitivity to lethal acid challenge, our previous work found that *L. monocytogenes* cells appeared to be injured after incubation at 48°C for 1 h as those heat adapted cells grew much slower compared to non-adapted control cells at 37°C (Shen et al., 2014). Therefore, the reduced survival of heat adapted cells may result from the injury triggered by sublethal heat treatment. We also found that the heat stress adapted *L. monocytogenes* cells exhibited cross protection to lethal alkaline stress by NaOH and KOH. Similar

observations were also reported by others which demonstrated that heat stress adaptation in *L. monocytogenes* induces cross-resistance to alkali based cleaners (Novak and Yuan, 2003; Taormina and Beuchat, 2001). Therefore, our data suggest that KOH and NaOH might not be suitable to be used to inactivate heat adapted *L. monocytogenes* cells.

H_2O_2 generates oxygen-free radicals that damages the cell membrane and disrupts the electron transport system. We observed stationary phase grown heat adapted *L. monocytogenes* cells were more sensitive to a lethal concentration of H_2O_2 compared to non-adapted cells which was similar to that observed by Lin and Chou (Lin and Chou, 2004) . In contrast, Lou and Yousef observed increased survival in 1000 ppm H_2O_2 in exponential-phase *L. monocytogenes* Scott A cells after pre-exposure to 45°C for 1 h (Lou and Yousef, 1997). These observations may be due to the differences in bacterial strains (Bug600 versus ScottA), the physiological state of *L. monocytogenes* (stationary phase versus exponential phase) or the differences in heat adaptation conditions (45°C versus 48°C). NaOCl is one of the most highly used disinfectants in food industry in which HOCl and HCl^- ions are the main active components responsible for creating oxidative stress (FUKUZAKI, 2006). Since our data showed that heat adaptation in *L. monocytogenes* resulted in increased susceptibility to H_2O_2, it is not surprising to see the increased susceptibility to another oxidizing agent NaOCl.

We observed that the heat stress adapted *L. monocytogenes* cells had greater sensitivity to quaternary ammonium compound-Lysol. Similar to these findings, Moorman et al. (Moorman et al., 2005) observed that heat adaptation in *L. innocua* resulted in increased sensitivity to a mixture of QACs. However, Lin et al. (2012) reported that *L. monocytogenes* heat adapted cells survived greater than non-adapted control cells in QAC (Lin et al., 2012). It is important to notice that Lin and co-workers prepared the heat adapted cells in PBS where the cells may be exposed to starvation instead of bacterial growth medium. Therefore, the observed increased resistance to QAC might result from starvation rather than heat adaptation. QACs exhibits the killing efficacy by interacting with bacterial cell membrane (Ioannou et al., 2007). Our previous study showed that *L. monocytogenes* cell envelope were thickened after being treated at 48°C for 60 min suggesting that modified cell membrane resulted from sublethal heat treatment could protect *L. monocytogenes* against QACs (Saha et al., 2015). However, Moorman et al. (Moorman et al., 2005) found that no membrane fluidity was changed after heat adaptation at 45°C in *L. innocua*. Therefore, the change of cell membrane proteins might contribute to the decrease survival to QACs. This hypothesis needs further investigation by comparing the proteome of cell membrane before and after heat stress adaptation.

Our findings show that the sublethal heat treatment at 48°C for 1 h enhanced the survival of *L. monocytogenes* cells in lethal concentrations of carvacrol and bay oil. Similarly, Ait-Ouazzou et al. (Ait - Ouazzou et al., 2013) reported that mild heat treatment at 45°C for 1 h protected *L. monocytogenes* cells against carvacrol inactivation. Several studies proposed that carvacrol exhibits bactericidal effect by damaging the cell membrane (Helander et al., 1998). Hence, the heat stress adapted *L. monocytogenes* may change the cell membrane composition during heat treatment which may minimize the interaction between carvacrol and cell membrane. In order to fully understand the heat stress conferred cross protection against carvacrol in *L. monocytogenes*, it is necessary to perform a comparative lipid composition analysis of the cell membrane before and after heat treatment at 48°C for 1 h. In addition, we noticed that heat stress adapted cells were still sensitive to red thyme and cinnamon. These distinct responses of heat adapted *L. monocytogenes* to different essential oils may be due to the different composition of these agents (Burt, 2004). Our data suggest that compared to carvacrol and bay oil, thyme and cinnamon may be better antimicrobial agents during food processing where heat adapted *L. monocytogenes* are present.

CONCLUSIONS

In conclusion, our findings demonstrate that the heat stress adaptation in *L. monocytogenes* did not result in increased resistance to lethal acid, oxidative agents, QAC, red thyme and cinnamon. However, NaOH, KOH, carvacrol and bay oil exhibited reduced killing efficacy when *L. monocytogenes* cells acquired heat stress adaptation. Therefore, the use of NaOH or KOH based alkaline disinfectants, and essential oils containing carvacrol and bay oil should be carefully

considered when heat adapted *L. monocytogenes* cells may be present.

ACKNOWLEDGEMENTS

This research was supported in part by Strategic Research Initiative and Food Safety Initiative awards to R. Nannapaneni from the Mississippi Agricultural and Forestry Experiment Station under project MIS-401160.

Conflict of Interest: There is no conflict of interest to declare

LITERATURE CITED

1. Ait‐Ouazzou, A., Espina, L., Gelaw, T., Lamo‐Castellví, S., Pagán, R., García‐Gonzalo, D., (2013). "New insights in mechanisms of bacterial inactivation by carvacrol". *J Appl. Microbiol*. 114, 173-185.
2. Burt, S., 2004. "Essential oils: their antibacterial properties and potential applications in foods—a review". *Int. J. Food Microbiol*. 94, 223-253.
3. Davidson, P.M., Harrison, M.A. (2002). "Resistance and adaptation to food antimicrobials, sanitizers, and other process controls". *Food Technology Champaign Then Chicago*-56, 69-78.
4. Doyle, M.E., Mazzotta, A.S., Wang, T., Wiseman, D.W., Scott, V.N. (2001). "Heat resistance of *Listeria monocytogenes". J Food Prot*. 64, 410-429.
5. Farber, J., Brown, B. (1990). "Effect of prior heat shock on heat resistance of *Listeria monocytogenes* in meat". *Appl. Environ. Microbiol.* 56, 1584-1587.
6. Ferreira, A., O'Byrne, C.P., Boor, K.J., 2001. "Role of ςB in Heat, Ethanol, Acid, and Oxidative Stress Resistance and during Carbon Starvation in *Listeria monocytogenes". Appl. Environ.Microbiol.* 67, 4454-4457.
7. Fukuzaki, S. (2006). "Mechanisms of actions of sodium hypochlorite in cleaning and disinfection processes". *Biocontrol science* 11, 147-157.
8. Gandhi, M., Chikindas, M.L. (2007). "*Listeria*: a foodborne pathogen that knows how to survive." *Int. J. Food Microbiol.* 113, 1-15.
9. Gray, M.J., Freitag, N.E., Boor, K.J., 2006. "How the bacterial pathogen Listeria monocytogenes mediates the switch from environmental Dr. Jekyll to pathogenic Mr. Hyde". Infection and immunity 74, 2505-2512.
10. Hamon, M., Bierne, H., Cossart, P. (2006). "*Listeria monocytogenes*: a multifaceted model". *Nat. Rev. Microbiol.* 4, 423-434.
11. Helander, I.M., Alakomi, H.-L., Latva-Kala, K., Mattila-Sandholm, T., Pol, I., Smid, E.J., Gorris, L.G., von Wright, A. (1998). "Characterization of the action of selected essential oil components on Gram-negative bacteria". *J. Agric. Food Chem.* 46, 3590-3595.
12. Hill, C., Cotter, P.D., Sleator, R.D., Gahan, C.G. (2002). "Bacterial stress response in *Listeria monocytogenes*: jumping the hurdles imposed by minimal processing". *Int. Dairy J.* 12, 273-283.
13. Ioannou, C.J., Hanlon, G.W., Denyer, S.P. (2007). "Action of disinfectant quaternary ammonium compounds against *Staphylococcus aureus". Antimicrob. Agents Chemother.* 51, 296-306.
14. Lee, I., Lin, J., Hall, H.K., Bearson, B., Foster, J.W. (1995). "The stationary‐phase sigma factor σ S (RpoS) is required for a sustained acid tolerance response in virulent *Salmonella* typhimurium". *Mol Microbiol*. 17, 155-167.
15. Lin, M.H., Chiang, M.L., Pan, C.L., Chou, C.C. (2012). "Heat shock and cold shock treatments affect the survival of *Listeria monocytogenes* and *Salmonella Typhimurium* exposed to disinfectants". *J Food Prot* 75, 695-700.
16. Lin, Y.-D., Chou, C.-C. (2004). "Effect of heat shock on thermal tolerance and susceptibility of *Listeria monocytogenes* to other environmental stresses". *Food Microbiol.* 21, 605-610.
17. Lou, Y., Yousef, A.E. (1997). "Adaptation to sublethal environmental stresses protects *Listeria monocytogenes* against lethal preservation factors". *Appl. Environ. Microbiol.* 63, 1252-1255.
18. Moorman, M., Nettleton, W., Ryser, E., Linz, J., Pestka, J. (2005). "Altered sensitivity to a quaternary ammonium sanitizer in stressed *Listeria innocua". J. Food Prot.* 68, 1659-1663.
19. Novak, J.S., Yuan, J.T. (2003). "Viability of *Clostridium perfringens*, *Escherichia coli*, and *Listeria monocytogenes* surviving mild heat or aqueous ozone treatment on beef followed by heat, alkali, or salt stress". *J. Food Prot.* 66, 382-389.

20. Ramaswamy, V., Cresence, V.M., Rejitha, J.S., Lekshmi, M.U., Dharsana, K., Prasad, S.P., Vijila, H.M. (2007). "*Listeria*-review of epidemiology and pathogenesis". *J. Microbiol. Immunol. Infect.* 40, 4.
21. Saha, S., Dhowlaghar, N., Lawrence, A., Nannapaneni, R., Sharma, C.S., Mahmoud, B.S. (2015). "Transmission electron microscopy study of *Listeria monocytogenes* serotype 1/2a cells exposed to sublethal heat stress and carvacrol". *J Miss Acad Sci.* 60, 300-304.
22. Shen, Q., Jangam, P.M., Soni, K.A., Nannapaneni, R., Schilling, W., Silva, J.L. (2014). "Low, medium, and high heat tolerant strains of *Listeria monocytogenes* and increased heat stress resistance after exposure to sublethal heat". *J. Food Prot.* 77, 1298-1307.
23. Skandamis, P., Nychas, G.J. (2001). "Effect of oregano essential oil on microbiological and physico‐chemical attributes of minced meat stored in air and modified atmospheres". *J. Appl. Microbiol.* 91, 1011-1022.
24. Smith-Palmer, A., Stewart, J., Fyfe, L. (2001). "The potential application of plant essential oils as natural food preservatives in soft cheese". *Food Microbiol.* 18, 463-470.
25. Soni, K.A., Nannapaneni, R., Tasara, T. (2011). "The contribution of transcriptomic and proteomic analysis in elucidating stress adaptation responses of *Listeria monocytogenes"*. Foodborne Pathog. Dis. 8, 843-852.
26. Taormina, P., Beuchat, L. (2001). "Survival and heat resistance of *Listeria monocytogenes* after exposure to alkali and chlorine". *Appl. Environ. Microbiol*. 67, 2555-2563.
27. Vasseur, C., Baverel, L., Hebraud, M., Labadie, J. (1999). "Effect of osmotic, alkaline, acid or thermal stresses on the growth and inhibition of *Listeria monocytogenes"*. *J. Appl. Microbiol.* 86, 469-476.
28. Yousef, A.E., Courtney, P.D. (2003). "Basics of stress adaptation and implications in new-generation foods".

UTILIZING BAYESIAN NEURAL NETWORKS TO MODEL THE OCEAN-ATMOSPHERE INTERFACE

Warith Abdullah, Remata Reddy, Cary Butler and Wilbur Walters
Department of Physics, Atmospheric Sciences & Geosciences
Jackson State University at Jackson
1400 J.R Lynch Street
Jackson, Mississippi 39217 USA

Corresponding Author: Warith Stone Abdullah, email: warith.i.abdullah@erdc.dren.mil

ABSTRACT

The ocean-atmosphere interface (OAI) is a dynamic boundary of complex energy and chemical exchange and is important to understand mechanisms that influence it. Research is on-going to improve how the OAI is represented within tropical cyclone (TC) prediction models and ensembles. Motivation for improvement stems from a rapidly changing thermodynamic environment caused by climate change. Such changes are not widely understood, as no scientist has observed or measured these changes on long time scales. We assert the possibility of climate change, its underlying uncertainties and modified atmospheric variability can potentially lead to rapid intensification. We argue simplification of OAI to capture model ensemble data uncertainty through probabilistic modeling via Bayesian Neural Network (BNN). We retrieved area- averaged satellite data from NOAA and NASA, created a data set of several parameters—atmospheric air temperature (AirTemp), atmospheric temperature anomaly (ATA), atmospheric carbon dioxide (CO_2), sea surface temperature (SST), tropical cyclone heat potential (TCHP), mid-layer wind shear (WindShear), convective available heat potential (CAPE), vertical motions (VerticalMotion), precipitable water content (PWC) and our derived OAI parameter as inputs into a BNN via R programming language. We used the BNN to model the OAI and inferenced potential favorability of an OAI given conditional probabilities. The BNN network rejected ATA and WindShear. Results showed probabilities acceptable within expert interpretations of parameter interactions to predict favorable OAI conditions.

Keywords: Tropical Storm, Bayesian Neural Network, Ocean-Atmosphere Interface

INTRODUCTION

Uncertainties in tropical cyclone (TC) intensification forecasting continue in modern-day forecasting models1. Recent storms such as TC Matthew (2016) and TC Irma (2017) demonstrated our limitations in predicting intensification, and rapid intensification events in a changing thermodynamic environment. A component of improving forecasting capabilities is representing the Ocean-Atmosphere Interface (OAI), also referred to as Air-Sea Interaction (ASI), within a model. Difficulties arise in resolving fluxes between atmosphere and ocean models to compute energetic and physical parameters within the interface. Research is underway to determine the model complexity necessary to simulate OAI1. On-going research suggests climate change as a primary driver behind the environmental behavior change. Abdullah et al., identified several atmospheric and oceanic physical parameters that comprise the OAI2. We attempt to extend the principle goal of establishing a technique to resolve the OAI by implementing a Bayesian Neural Network (BNN, or Bayesian Belief Network) statistical model. We treat the OAI holistically, thus our approach will linearize the physical parameters to simplify the model. We tabularize decadal data from several physical parameters within the Gulf of Mexico (GOM) domain to build the BNN and make a probabilistic prediction of the OAI magnitude.

INTRODUCTION

Ocean-Atmosphere Interface (OAI). In general, large scale modeling of the ocean and atmosphere involves many complex physical equations, multi- dimensional regression and other techniques[3]. Such techniques are inherently nonlinear to resolve physics, energy and chemical fluxes across various boundary solutions. A model ensemble is required to model a tropical cyclone, generally comprising of atmospheric, oceanic and vortex models[3]. Generally, solutions from one model are passed, given established boundary conditions, to generate a tropical storm. The OAI exchange of fluxes occurs at the interface of ocean atmosphere boundary and through compensatory dynamical circulations that maintain the observed climate of the planet[3]. However, representing the interface of energy flux between the ocean and atmosphere is either poor or non-existent[1,3]. This interface is important to understand both cyclogenesis and intensification.

OAI Current Implementation. Current schemes to represent the OAI include the Message Passing Interface Princeton Ocean Model for Tropical Cyclones (MPIPOM-TC)[3] in an ensemble, like that of NOAA Hurricane Weather Research Forecast model (HWRF). Energy exchanges occur at the flux boundary of a statistically accurate sea surface temperature (SST) field as input into the model. Issues arise for both coupled and uncoupled schemes. An uncoupled hurricane model with a static SST field is restricted by its inability to account for SST changes during model integration, which can contribute to high intensity bias[4]. A hurricane model coupled to an ocean model that does not account for fully three-dimensional ocean dynamics may only account for some of the hurricane-induced SST changes during model integration[5].

OAI Linearization. As expressed by Pond et al., the OAI is a highly coupled, non-linear system that should be treated as a single entity[6]. We attempt to simplify the OAI by treating it as a holistic, linear system, primarily to address uncertainties. To this end, this paper hypothesizes the effectiveness of treating the OAI linearly with ocean and atmosphere physical parameters to represent scalar magnitudes of the OAI. Additionally, we investigate whether a linearized OAI model can assist a TC ensemble to improve TC intensification prediction (Figure 1).

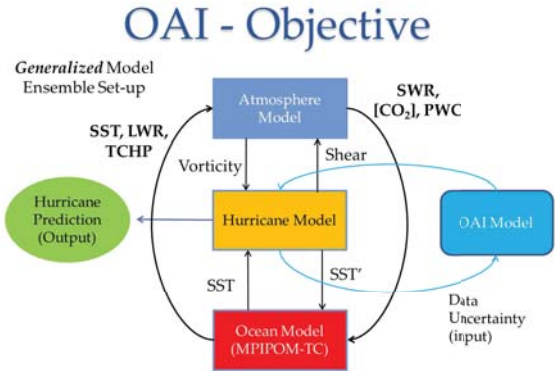

Figure 1. Generalized Model Ensemble set-up with OAI Model as an uncertainty resolver.

Data

Description. In efforts to understand causal impacts of varying atmospheric and ocean parameters that comprise the OAI, a dataset was constructed specifically for statistical models to draw inferences of causal impacts and their potential relationships. We assumed no time or space dependency and considered only magnitudes of each parameter. We concentrated on measurements from the GOM basin, primarily due to high TC activity. Each value is taken as an area-averaged measurement (except for Convective Available Potential Energy or CAPE at the time this study was conducted) for the period of August, September and October for each year, resulting in three data points per year over twelve years. The geospatial range of study within the GOM basin is approximate max-min latitude 31°, 23° respectively; approximate max-min longitude 97°, 83° respectively.

Sources. We collect data from multiple resources including NOAA National Centers for Environmental Information (NCEP), NOAA Atlantic Oceanographic and Meteorological Laboratory (AOML), NOAA Earth System Research Laboratory (ESRL), the National Hurricane Center (NHC), the Cooperative Institute for Meteorological Satellite Studies (CIMSS) join project with the University of Wisconsin-Madison, and the University of Wyoming Department of Atmospheric Science.

Parameter Description. Atmosphere Temperature Anomaly (ATA) is the mean temperature in degrees (°C) averaged monthly per year relative to 1951-1980 base period and is represented as a double-precision number. Atmospheric Temperature (AirTemp) is the mean temperature in degrees (°C) averaged monthly via NCEP/NCAR reanalysis forecast system performing data assimilation using data from 1948 to present[8] and is represented as a double-precision number. Atmospheric Carbon Dioxide (CO2) is the monthly averages of atmospheric carbon dioxide (ppm) via NOAA ESRL Global Monitoring Division at Mauna Lao[10] and is represented as a double-precision number. Convective Available Potential Energy (CAPE) is the "area averaged" CAPE (Joules kg-1) via University of Wyoming[9] and is represented as double-precision number. Tropical Cyclone Heat Potential (TCHP) is the area/monthly averaged TCHP (kJ cm-2) via NOAA AOML[11] and is represented as a double-precision number. Sea Surface Temperature (SST) is the monthly mean SST (°C) via International Collaborative Ocean-Atmosphere Dataset (ICOADS)[12] and is represented as a double-precision number. Preciptiable Water Content (PWC) is the mean water content precipitated from a column of air (kg m-2) via NCEP/NCAR reanalysis forecast system performing data assimilation using data from 1948 to present[8] and is represented as a double-precision number. Mid-layer Atmospheric Wind shear (Windshear) is the mean mid-level atmospheric wind shear (the change in wind speed and direction with height) via University of Wisconsin and the CIMSS[13], numeric format. Vertical Motions (VerticalMotion) is the vertical motion updrafts (m s-1) via University of Wyoming[9] and is represented as a double-precision number. OAI is the three-category representation of the state of the OAI, given the probability of all other parameters and is represented as a string format.

Uncertainties. Data collection devices (sensors, satellites, buoys etc.,) are subject to the elements and other factors and data retrievals are not always consistent. Therefore, missing data is an obvious limitation. Statistical techniques in data interpolation and extrapolation are necessary to overcome these limitations. The extents to which these techniques are implemented depend on many constraints surrounding length of time, sparseness, if the data is sufficient enough to interpolate from and the availability of previous data to allow for extrapolation.

METHODS

Bayesian Neural Network (BNN). Bayesian Belief Networks or Bayesian Neural Networks are easily implementable statistical models that capture reasoning given uncertainty from data by either utilizing evidence from other data, domain expertise or both14. For this reason, we identified Bayesian statistical modeling as a novel approach to stochastic predictions within a complex system, as identified by Berliner, Royle, Wikle and Milliff (1998)15. Knowledge of the modeled domain is contained within directed-acyclic-graphs (DAGs), where each node contains a conditional probability table (CPT). BNN utilize inferencing to derive insights between nodes. For example, if we can infer node C from node A with certainty (x), and we can infer node C from node B with certainty (y), what can we conclude on the certainty of node C? The certainty of node C will be a probabilistic calculation.

BNN requirements. A BNN requires that the network contain a set of nodes (or variables) and a set of directed edges between nodes. Further, such networks are restricted from containing cycles. Nodes and their connected edges form a DAG (figure. 2), whereby each node has a finite set of mutually exclusive states. Each node A with parents B1,…Bn is an attached CPT given by $P(A|B1,\ldots Bn)$.

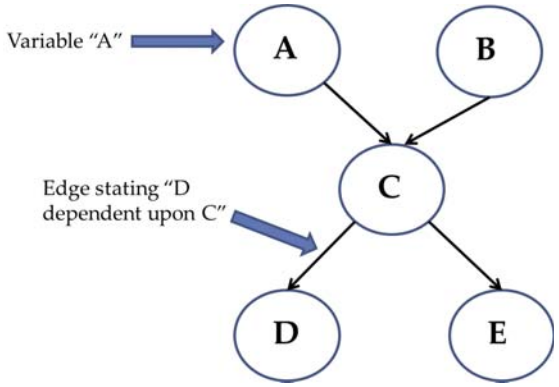

Figure 2. General DAG diagram.

Bayes Theorem. Each node within a DAG contains a CPT built upon Bayes Theorem, which states the probability of an event based upon prior knowledge of conditions that might be related to the event[14]. The basic property for conditional probability, known as the posterior distribution, is given as,

$$P(A|B) = \frac{P(B|A)P(A)}{P(B)} = \frac{P(A \wedge B)}{P(B)} \quad \text{eq. 1}$$

where the Joint-Probability distribution to build joint probability tables (JPTs) for A and B is the product of the prior P(A) and sampling P(B|A) distributions, given as,

$$P(A \wedge B) = P(B)P(B|A) \quad \text{eq. 2}$$

The property for marginalization of a parameter within a DAG is,

$$P(A) = \sum_B P(A \wedge B) \quad \text{eq. 3}$$

Updating joint-probabilities is the product of the quotient of the initial joint probability and the prior distribution of the "evidenced" parameter and the distribution of evidence. The property is given as,

$$P^*(A \wedge B) = \frac{P(A \wedge B)}{P(A)} P^*(A) \quad \text{eq. 4}$$

Implementation. We utilize the statistical programming language, R, and supporting modules to perform data preprocessing and construct the BNN.

Data Preprocessing. We tabularized the data into a dataframe of 37 rows and 10 columns and performed a normalization scheme within the interval (0, 1]. We set zero values equal to 0.01 due to interpreter formatting errors when splitting the data into categorical values. The values were randomized to prevent model fitting to the structure of the data. A correlation matrix was built to evaluate statistical significance between the parameters (Figure 3). The parameter AirTemp shows weak correlation with atmospheric CO2, despite domain knowledge confirming the opposite. AirTemp is also weak with respect to SST, which again is the opposite of common domain knowledge. Parameter WindShear shows larger weak correlation, again, behaving contrary to domain knowledge against all physical parameters. We removed the AirTemp parameter and constructed another matrix, given in figure 4.

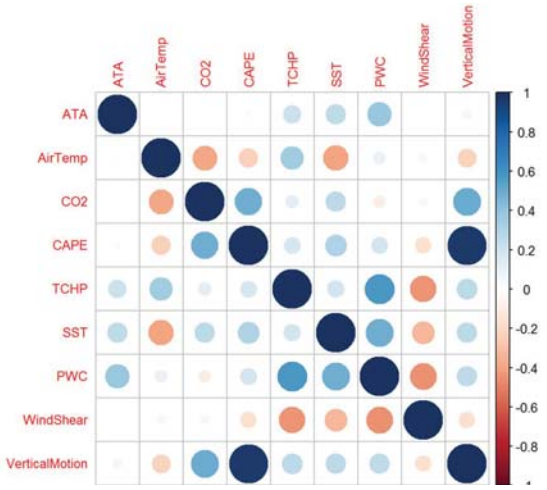

Figure 3. Initial correlation matrix for dataframe.

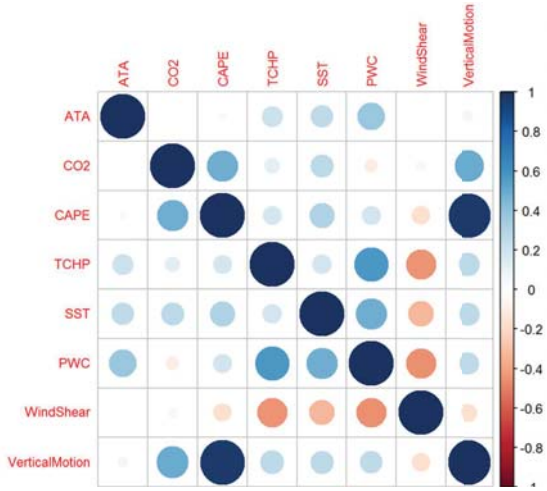

Figure 4. Second correlation matrix, parameter "AirTemp" removed.

The second matrix shows noticeable improvements, although the parameter WindShear continues to be estimated with very weak correlation with respect to TCHP, SST and PWC. We decided to leave WindShear within the dataframe to build the BNN under the assumption the model, given linear dependency from Bayes Theorem, would exclude it.

Constructing the BNN. R programming supports a module named "bnlearn" and we utilized it to construct the BNN. The module contains DAG

building methods such as Iterative Associate Markov Blanketing, Hill-Climb and others. We implemented the Hill-Climb algorithm. To build CPTs, bnlearn calls the "fit" method. JPTs are built and inferencing between nodes is done by calling the "cpquery" method. We take our dataframe and convert it into numeric intervals (0, 0.3, 0.7, 1.1) and further, create categorical labels from 1 to 3. The min-max thresholds 0 and 1.1 respectively of the numeric interval were chosen to abide by formatting rules within the R programming interpreter to appropriately split the data. Because the minimum of the data was programmatically set to 0.01, we could split the data on a minimum—zero. Additionally, the data maximum is 1, therefore we could split the data at a categorical maximum—1.1.

Initial BNN. The initial BNN (Figure 5) contains two separate DAGs. The left DAG contains parameter OAI as a base node, the remaining DAG with parameter SST as the base node. The BNN did not consider either ATA or WindShear as statistically significant parameters and it agrees with the results of the second correlation matrix. Further, no CPTs of parameters ATA and WindShear are linearly related with respect to any DAG.

Second BNN. We removed ATA and WindShear and rebuilt the BNN (Figure 6). The previous DAGs maintain their structure, however, the CAPE and PWC parameters are related to each other and incorrectly remain separated. The state of the BNN is incomplete, as we will not be able to generate inferences between all nodes.

Completed BNN. CAPE is physically related to PWC. As PWC increases, latent heat of evaporation also increases and contributes to the available potential energy of an air parcel (Abdullah, et al)[2]. BNNs collect information from uncertainty within data, expert (or domain) knowledge, or both. In this case, we know CAPE and PWC are related, therefore, we use this information to construct our completed BNN (Figure 7) by adding an edge between CAPE and PWC.

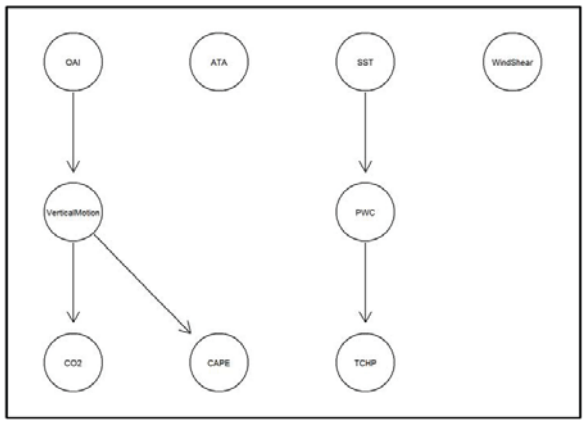

Figure 5. Initial BNN. Two DAGs are constructed, two parameters, ATA and WindShear, are not considered.

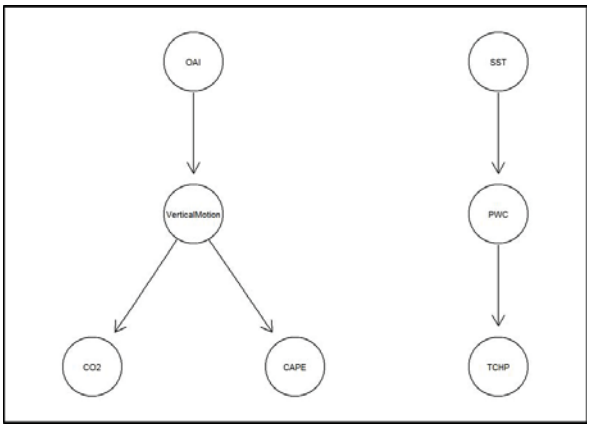

Figure 6. Second BNN configuration. Two DAGs remain as originally built, ATA and WindShear are removed.

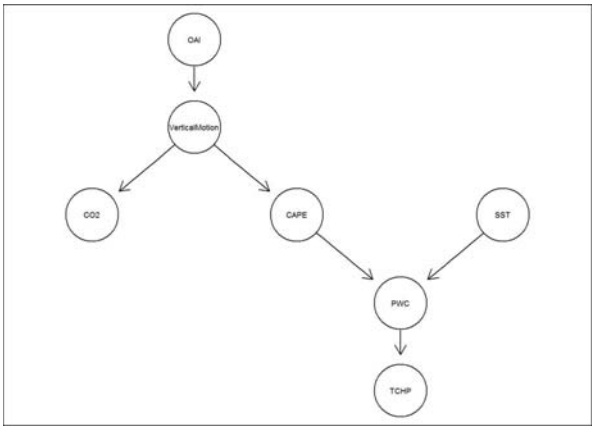

Figure 7. Expert inferred completed BNN. An edge is added between CAPE and PWC parameters.

RESULTS

BNN Cpquery First Output. Now we draw inferences from our BNN by process of probabilistic query. Our initial R syntax Cpquery asks, "what is the likelihood that low CAPE, mid TCHP, mid PWC, mid Vertical Motion, and low atmospheric CO2 can predict a moderately favorable OAI?" (Table 1). We computed a result of 0.6612903, or approximately a 66 percent probability that a moderately favorable environment to support TC development or intensification can occur given the physical parameter conditions.

BNN Cpquery Second Output. To ensure stability of the model output, we ran another R syntax Cpquery. "what is the likelihood that low CAPE, midTCHP, mid PWC, mid Vertical Motion, low atmospheric CO2 and low SST can predict a
moderately favorable OAI?" (Table 1). We computed a result of 0.85, or approximately an 85 percent probability that a moderately favorable environment to support TC development or intensification can occur given the physical parameter conditions.

CONCLUSIONS

Our approach to linearizing the OAI given a BNN provided insight into what we understand theoretically about OAI behavior. The BNN demonstrated sensitivity parameterizing, verifying that small changes in the system can produce considerable changes. Further, it is feasible to implement a large-scale BNN, however, problems may arise in data integration (i.e., model generated data versus raw observations) given the assumptions we used. Acquisition of a larger, higher-resolution data set is in progress to continue testing and verifying our BNN. Given our data set was relatively small, parameters ATA, WindShear and AirTemp were too coarse in variance, therefore were not considered statistically significant. This narrow variance is a product of the coarse resolution from NOAA/NCEP reanalysis maps, which are global in scale, whereas our domain is the GOM. Data for the WindShear parameter was retrieved for mid-layer atmosphere winds (850 – 500 mb), and we considered capturing features near sea level (1000 – 850 mb) in our continued research. Alhough the parameters have been linearized for the BNN, it must represent the OAI complexity in terms of parameters that exist. In future study, we will add additional physical conditions to the BNN. Finally, the OAI category must represent this order of complexity. We are developing a heuristic over our expanding dataset using machine learning algorithms to classify various magnitudes of the OAI.

LITERATURE CITED

1. Soloviev, A.V., Lukas, R., Donelan, M.A., Haus, B.K., Ginis, I., 2014: The air-sea interface and surface stress under tropical cyclones. *Scientific Reports.,* **Vol 4** 5306.
2. Abdullah, W.S., Reddy, R., Heydari, E., Walters, W., 2016: A Study of Large-Scale Surface Fluxes, Processes and Heavy Precipitation Associated with Land Falling Tropical Storm Lee over Gulf of Mexico using Remote Sensing and Satellite Data. *Mississippi Academy of Sciences.,* **Vol 62.**
3. Tallapragada, V., et al 2014: Hurricane Weather Research and Forecast (HWRF) Model 2014 Scientific Documentation. *NOAA/NWS/NCEP.*
4. Bender, M. A. and I. Ginis, 2000: Real case simulation of hurricane-ocean interaction using a high-resolution coupled model: Effects on hurricane intensity. Mon. Wea. Rev., 128, 917-946.
5. Yablonsky, R. M. and I. Ginis, 2009: Limitation of one-dimensional ocean models for coupled hurricane-ocean model forecasts. Mon. Wea. Rev., 137, 4410–4419.
6. Pond. S., 1972: The Exchanges of Momentum, Heat and Moisture at the Ocean-Atmosphere Interface. *Numerical Models of Ocean Circulation, National Academy of Sciences Proceedings.* **Oct. 17 – 20,** 26 – 38.
7. GISTEMP Team, 2016: *GISS Surface Temperature Analysis (GISTEMP)*. NASA Goddard Institute for Space Studies. Dataset

accessed 2016-11-15
at http://data.giss.nasa.gov/gistemp/.

8. The NCEP/NCAR 40-Year Reanalysis Project: March, 1996 BAMS

9. University of Wisconsin – CIMSS. Data accessed 2016-11-15 at
http://tropic.ssec.wisc.edu/tropic.php

10. NOAA ESRL Global Monitoring Division at Mauna Lao, Hawaii. Data accessed 2016-11-15 at
http://www.esrl.noaa.gov/gmd/ccgg/trends/graph.html

11. NOAA AOML. Data accessed 2016-11-15 at
http://www.aoml.noaa.gov/phod/cyclone/data/fulllist.html

12. NOAA ESRL ICOADS Dataset. Data accessed 2016-14-11 at
http://www.esrl.noaa.gov/coads/coads_cdc_netcdf.shtml

13. University of Wyoming Department of Atmospheric Science soundings. Data accessed 2016-14-11 & 2016-15-11 at
http://weather.uwyo.edu/upperair/sounding.html

14. Finn V. Jensen. An Introduction to Bayesian Networks. UCL Press, 1996. Chap. 2.

15. Berliner, M.L., Royle, A.J., Wikle. C.K., Milliff. R.F., 1998: Bayesian Methods in the Atmospheric Sciences., *Bayesian Statistics*. **Vol 6,** 66-100.

ENVIRONMENTAL MODELING AND PREDICTION FOR CLIMATE AND SEASONAL FLUCTUATIONS OVER GRAND BAY OF GULF OF MEXICO

R. Suseela Reddy[1], Duanjun Lu[1], Mehri Fadavi[1], Paul Tchounwou [1] and Paulinus Chigbu [2]

[1] Jackson State University, Jackson, MS 39217
[2] University of Maryland Eastern Shore, 21853

Corresponding Author: R. Suseela Reddy, E-mail: remata.s.reddy@jsums.edu

Abstract: The Gulf of Mexico region is prone to severe weather events throughout the year and is affected due to environmental changes over the coastal regions (ex. flooding and sea breeze circulations, tropical cyclones/hurricanes, ENSO etc.). Understanding, modeling and predicting weather/climate dynamics and meteorological coastal processes for the Gulf region is important for agriculture, fisheries and forestry management as this region is of interest for the country's economy and social aspects. Our goal is to investigate the seasonal patterns of meteorological parameters in order to predict their impacts on ecosystem and fish populations over the Grand Bay National Estuarine Research Reserve (GBNER) area using the Penn State/NCAR Mesoscale Model (MM5). In the present study, the MM5 version 3 Weather/Environmental model was run using data assimilation techniques where non-conventional data from various sources are fed into the model as initial and lateral boundary conditions to simulate seasonal variations of surface features and precipitation. Other simulation parameters include sea surface temperature, sea level pressure and surface wind magnitude. The climatic and seasonal fluctuations of these parameters have important implications for the GBNERR ecosystem.

Keywords: Grand Bay, Environmental modeling, Seasonal climate prediction, Ecosystem, Fish population

INTRODUCTION

The Grand Bay Reserve is one of the most biologically productive estuarine ecosystems in the Gulf of Mexico region, supporting several rare or endangered plant and animal species, numerous important marine fishery resources, diverse habitat types and important archaeological sites. The reserve is of major ecological significance because of its diverse range of habitats. It encompasses coastal bay, expansive saltwater marshes, maritime pine forest, pine savanna and pitcher plant bogs. It supports extensive and productive oyster reefs and sea grass habitats. It serves as nursery area for many of the Gulf of Mexico's important recreational and commercial marine species, such as shrimp, blue crab, speckled trout, red fish. The area is used for recreational and commercial fishing, birding and aesthetic enjoyment (Fig.1).

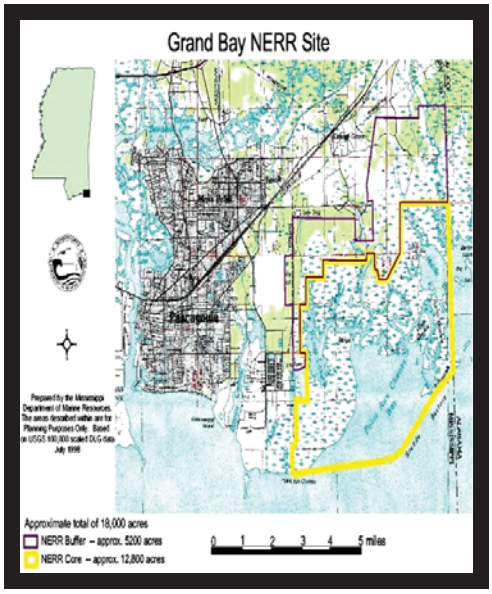

Figure 1: Grand Bay National Estuarine Research Reserve (GBNER)

Previous studies (Chigbu et al., 2004; Chigbu et.al., 2005) showed an evidence of climate and seasonal fluctuations over the Gulf region including Mississippi Sound and Grand Bay areas and discussed the impacts of such variations on the ecosystem and shellfish management.

In the present study, we investigate to study the climate and seasonal fluctuations of meteorological parameters of temperature, precipitation, surfaces fluxes, sea level pressure, wind and etc over the Grand Bay of Gulf of Mexico using environmental modeling MM5. We conduct seasonal prediction and impact assessment on ecosystem of fish population over the Grand Bay area and compare model output with observations.

MATERIAL AND METHODS

Model Overview

MM5 model has been developed for almost 30 years and the latest version released is version 3. This is a fairly sophisticated modeling system with full and explicit microphysics, a non-hydrostatic formulation, soil and vegetation parameterization and multiple nesting capabilities. The model consists of five modules: TERRAIN, REGRID, RAWINS/LITTLE_R, INTERPF and MM5. Of this entire set of programs, the MM5 module itself is the actual numerical weather prediction part of the modeling system (Figure 2). The output of the model was viewed using a graphical package GrADS (Gridded Analysis and Display System). Actual information on the MM5 model can found at www.mmm.ucar.edu/mm5/mm5home.html (Grell et.al., 2003; Kain et.al., 1993)

Terrain

The TERRAIN module creates input terrain elevation and vegetation (land use) data for each grid directly from source input datasets and horizontally interpolates (or analyzes) from a latitude/longitude mesh onto a chosen mesoscale gird. The main tasks for TERRAIN are: (i) select subsets of terrain and land use/cover data that covers a given model domain, (ii) create fields of topography and land use/cover either by interpolation or by objective analysis at domain grid points, (iii) reset topography and land use/cover data on nest grid boundaries and adjust them for overlapping nests, (iv) computes constants fields, such as latitude and longitude for each grid point for a given grid, map scale factor and Coriolis parameter.

The input TERRAIN requires information about model domain dimensions (number of grid points and grid spacing) for each required grid. In addition, terrain and land use/cover data are required. There are several types of input datasets available in the MM5 model package for TERRAIN, which include: terrain elevation, land-use/vegetation, land-water mask, soil types, vegetation fraction and deep soil temperature.

They differ in coverage and horizontal resolution. All data are available at six resolutions at 1 degree, 30, 10, 5, and 2 minutes, and 30 seconds. Each dataset recognizes 13 types of land use/cover ranging from urban to tropical forest.

Regrind

REGRID is the second module and it consists of two parts: pregrid and regridder. REGIRD handles pressure levels and surface analyses, and two-dimensional interpolation. The main task of pregrid is to extract data from appropriate NCAR archived gridded meteorological analyses (NCEP or ECMWF) that correspond to user determined time intervals that the user will be running. Resulting extracted files are used as inputs in regridder, the second part of the REGRID module. Regridder recombines data created by TERRAIN and REGRID/pregrid modules resulting in one data file for each nested grid domain. TERRAIN data includes information about domain size and topography; REGRID/pregrid provides atmospheric data that have at least these variables: sea-level pressure, horizontal wind components, temperature, relative humidity, height of pressure levels, sea-surface temperature and snow-cover data and times covering MM5 model simulation. Other data levels may be used as well, interpolated and passed on to the modeling system. REGRID/regridder will merge both data adjusting for topography and sea surface temperature (if applicable). Output from REGRID/regridder will be used as the first guess to an objective analysis (RAWINS/LITTLE_R), or as analyses which are to be directly interpolated to the MM5 model levels for initial and boundary conditions for MM5 (INTERPF). In short, pregrid handles data input task and regridder handles horizontal interpolation to the MM5 grid.

Rawins/Little_R

Either RAWINS or LITTE_R module is run depending on user preference. LITTLE_R is alternative to RAWINS that was used in this case. This module provides input of upper atmosphere and surface observations. It reads rawinsonde and surface observation data from NCAR archive and extracts stations within modeling domains and simulation time. Its main function is to enhance the first-guess meteorological data or the low-resolution analyses output with observations. The first-guess could be either from REGRID or MM5 module. The goal is to improve coarse resolution of gridded data, which is typically 2.5 x 2.5 degree by including either rawinsonde or surface data. This may be important for model run over limited areas where gridded data cannot resolve horizontal and vertical variability at model domain's resolution. Neither vertical interpolation nor temporal interpolation is done by LITTLE_R and strictly gridded data alone is used for observational analysis. This module is optional and the data are not required for MM5 model run. The output data produced is on pressure-level.

Interpf

INTERPF is the last module that processes input data before running MM5. Typically the modeling system gets and analyzes data on pressure surfaces, but these have to be interpolated to the model's vertical coordinate before being input into MM5.

The output data generated by the preprocessors: REGRID/regridder or RAWINS/LITTLE_R for input are pressure-level meteorological fields, which are vertically interpolated into sigma levels. The sigma levels are user defined model sigma levels. INTERPF provides initial, lateral, and lower boundary conditions for each grid (main and nested).

MM5

MM5 calculates all required variables at each grid point during the time of simulation. The adopted grid is Arakawa B-grid staggered mesh that consists of dot (corner) and cross (center) grid points where vector and scalar data are defined respectively. In this module a user can specify various physical options and parameterizations. Different schemes could be used for different nesting, but it is better to keep the same for all.

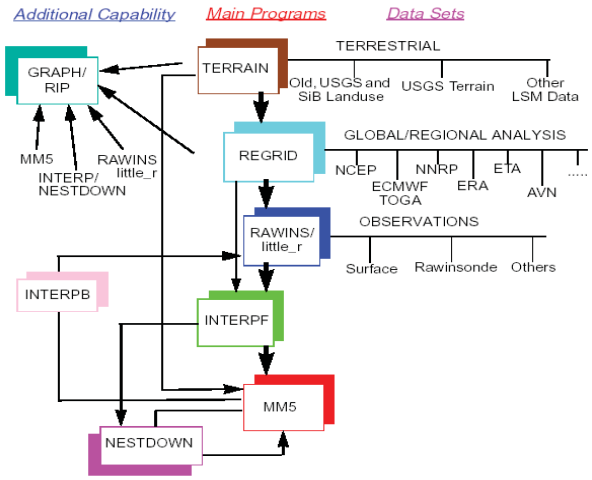

Figure 2: MM5 Modeling System Flowchart

Model Configuration

The major physics options include the following and are given in Table1.

(i)Microphysics: Explicit moisture schemes and Cumulus parameterization represents sub grid scale vertical fluxes and rainfall due to convective clouds (Krishnamurti et.al., 1998).

(ii)PBL schemes (Planetary Boundary Level)

(iii)Radiation Schemes

(iv)Surface Schemes provide sensible and latent heat flux effects of land and water surfaces.

The model runs using two-nested scheme with outer domain resolution of 27km and fine domain resolution of 9km and 3km. For seasonal climate fluctuations, the simulation periods include 2003 summer (from July to September) and 2003-2004 winter (from December 2003 to February, 2004). For surface fluxes and associated weather patterns, the simulated periods include for winter 2002 (14-15 January, 2002) and for summer 2002 (18-19 June, 2002).The investigated results will primarily focus on the output from higher resolution domain (9km and 3km). To make the investigation direct and simplification, only a sub-section of fine domain which located over Grand Bay and its surrounding areas is presented here in Table 1.

Table 1: MM5 Configuration

MM5 Configuration - 48hr simulation - 23 σ levels				
Global Analysis	ADP FNL Observations	Domain		
		1	2	3
Physics		27km	9km	3km
Microphysics		Dudhia Simple Ice		
Cumulus Scheme		Kain-Fritsch 2		
PBL Scheme		Blackadar PBL		
Radiation		RRTM Longwave and Dudhia Shortwave		

RESULTS AND DISCUSSION

The MM5 model outputs for meteorological variable which include surface temperature, surface wind speed, seasonal rainfall and surface fluxes are given in Figures 3 to 10. The model output comparisons with observations are given in Table 2.

Surface temperature

During the warm season, the MM5 provided a warm bias over the land and ocean surface (Fig. 3), with the range from 1.0 C to 1.7 C. The

temperature anomalies are bigger over land than the ocean surface. These biases are not just an artifact of post-processing because the temperature mean error at lowest half-sigma level also demonstrated a warmer bias over the land of domain (not shown). During winter, the model presents a warm bias for surface temperature forecast as well. But the magnitude of bias is smaller than that during summer with the range from 0.1 C to 1.1C.The interesting distribution of anomalies during winter seems to reverse the pattern during summer. For example, a warm center is over water and very slight warm biases over land during winter. The time series of surface temperature provided an evident of over prediction during summer. But during winter, the model does not yield a constant warm bias of domain averaged surface temperature. In many cases, the model produced a cool temperature bias resulting in the weak warm bias as discussed or a slight warm bias (Fig. 4).

Surface wind speed

During the warm season, an evident of high wind speed bias appeared across the domain of the MM5 with the average of 1.34 m/s during summer (Fig. 5a). During winter (Fig.5b), there is an over prediction center located in the Mobile County, AL. The positive wind speed bias is not strong as that during summer. The weaker wind speed bias during winter may be related to the surface temperature bias. The time serial output of surface wind speed also provides higher wind speed during both summer and winter season (not shown).

Seasonal rainfall

During warm season, the MM5 yielded the seasonal precipitation in most areas with a magnitude of 30 mm to 210 mm over land (Fig. 6a). The observed rainfall (Fig. 6b) was substantially greater than forecast rainfall ranging from 240 to 500 mm. The under prediction of precipitation may result from the coarse initial condition (1 degree AVN used as initial conditions), the lack of real time sea surface temperature ingestion, and the insufficiency of model physical processes. Another feature of the seasonally forecasted rainfall is the existence of the significant local variation produced by the MM5, which is not apparent in the observations. During cool season (Fig. 7), the observed precipitation only has about half magnitude of that during summer. In most areas over land, the precipitation was about 100 mm to 140 mm while over the ocean surface, the seasonal rainfall ranged from 160 mm to 240 mm. The MM5 over forecasted the seasonal rainfall over land whereas it under predicted rainfall over ocean. The time series outputs of domain averaged rainfall (Fig.8) also reveal that the MM5 model under forecast during summer. It is noticed that many precipitation cases is not simulated from model. During winter, the models obviously improve its performance on precipitation. The model produced a comparable amount of 24h accumulative rainfall with a slight over prediction

Surface fluxes

The sea level pressure is low during winter with an average of 1005 mb and high during the summer with an average of 1009 mb The heat fluxes are high during January with an average of 80 W/m^2 compared to July with an average of 30 W/m^2 The precipitation is maximum over the Grand Bay during January with a maximum of 1.85 cm compared to July with a maximum of 0.5 cm. Sea surface temperatures during the winter is low compared to summer over the Grand Bay region. The environmental model captured the seasonal variations and model output is in good agreement with observations (Figures 9 to 12). The MM5 model was widely used for better understanding of coastal processes, land falling hurricane intensity and track forecast, land-sea breeze circulations and ocean-atmospheric interactions and flood forecasting (Reddy et.al., 2003; Reddy, 2002; Reddy et al., 2009); Reddy et.al., 2009; Remata et.al., 2003). Understanding, modeling and predicting weather/climate dynamics and seasonal fluctuations of meteorological coastal processes for the Gulf region and important for fisheries and ecosystem management as this region is of great interest for the country's

economy and social impacts.

The meteorological information for the Grand Bay NIRR can be used (i) to provide atmospheric data and platform for estuarine research at the reserve, (ii) to give meteorological context (atmospheric forcing) for long-term environmental programs at the reserve, (iii) to observe and characterize important events such as storms, heat and cold waves, droughts and heavy rainfall, and (iv) to detect trends and characterize climate variability over the long-term. Climate and seasonal fluctuations in surface heat and latent fluxes over the Gulf of Mexico and associated heavy precipitation during land-falling storms were observed (Wang et.al., 2001; White et.al., 2001) and over the Grand Bay and their impacts on the ecosystem and inhabitants were reported (Chigbu et.al., 2005).

3.1. Tables and Figures

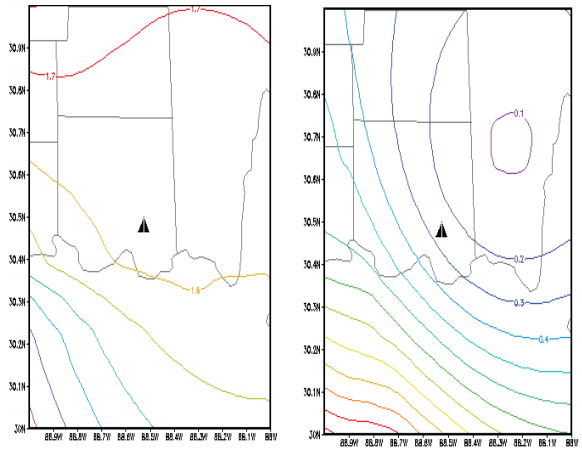

a) b)

Figure 3. Surface temperature biases during (a) summer and (b) winter. The intervals of contours are both 0.1 C for summer and winter. The triangle is the location of Grand Bay region.

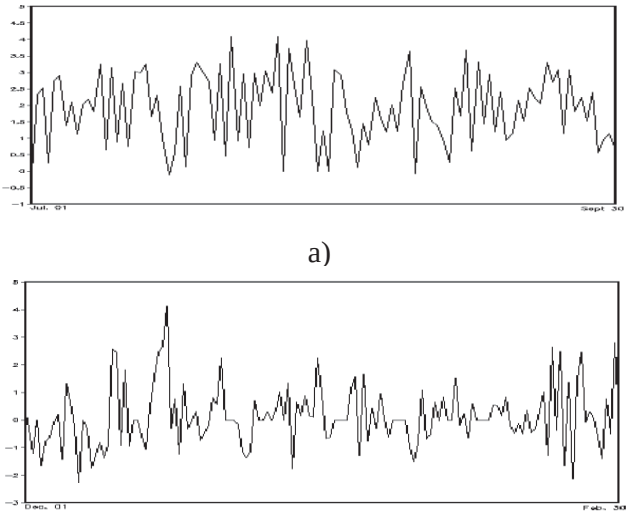

a)

b)

Figure 4.Time serial domain-averaged surface temperature biases (a) during summer and (b) winter.

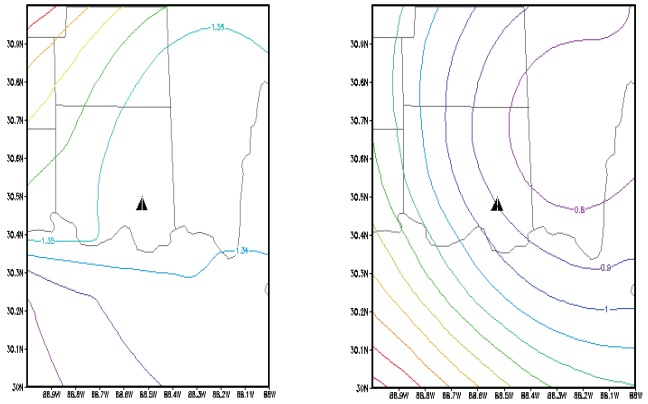

a) b)

Figure 5. Surface wind speed biases during (a) summer (b) winter

Jan	Wind		Temperature	Total
18	Ave.	V. Dir.	Mean	Precip.
	mph	Deg	Deg. F.	inches
Total				1.91
Ave.	4.9	133	58	
Max.			62	
Min.			50	

Jan	Wind		Temperature	Total
19	Ave.	V. Dir.	Mean	Precip.
	mph	Deg	Deg. F.	inches
Total				0
Ave.	3	237	59.8	
Max.			74	
Min.			53	

Jul	Wind		Temperature	Total
14	Ave.	V. Dir.	Mean	Precip.
	mph	Deg	Deg. F.	inches
Total				0.26
Ave.	2.3	191	83.1	
Max.			95	
Min.			73	

Jul	Wind		Temperature	Total
15	Ave.	V. Dir.	Mean	Precip.
	mph	Deg	Deg. F.	inches
Total				0.19
Ave.	2.5	200	85.2	
Max.			97	
Min.			75	

Table 2: Grand Bay Station Data for 2004

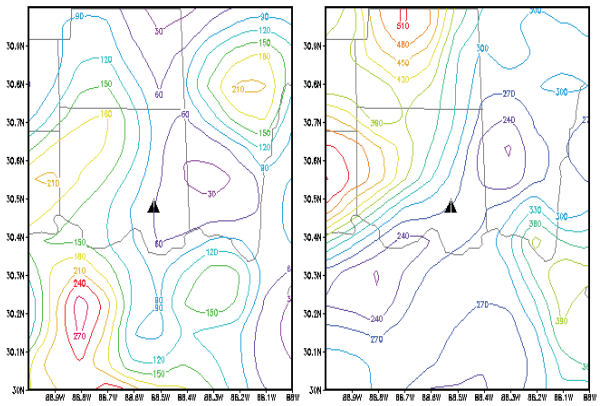

Figure 6. Seasonal rainfall (mm) during (a) summer from observation and (b) MM5 simulation

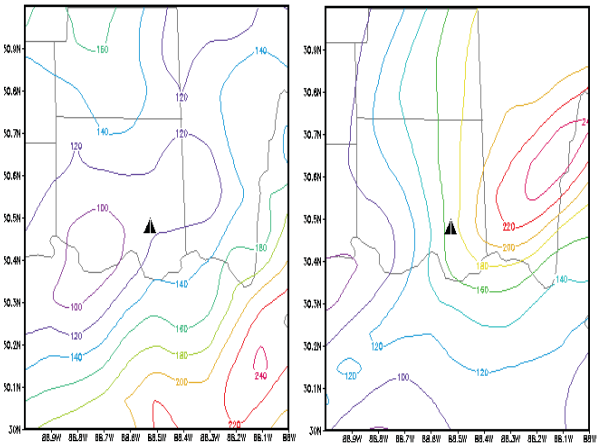

Figure7. Seasonal rainfall (mm) during winter from (a) observation and (b) MM5 simulation

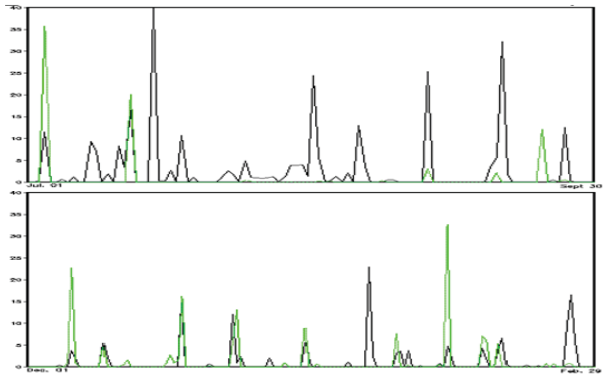

Figure 8. Time series of average rainfall (mm) from observation (solid) and MM5 simulation (dashed) during (a) summer and (b) during winter

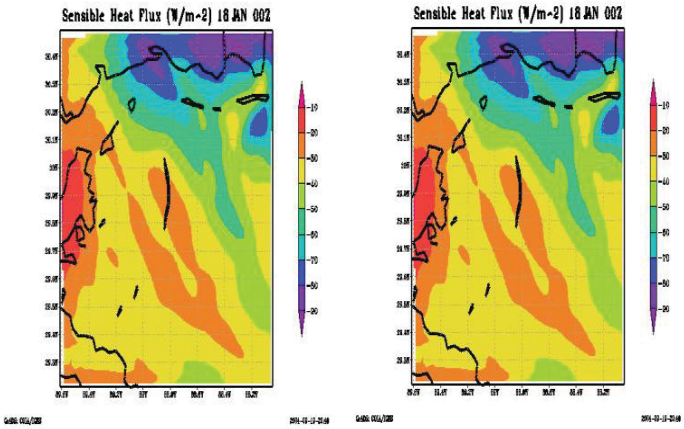

Figure 9. Sensible heat flux for (a) Januaruy18 and 19, 2004

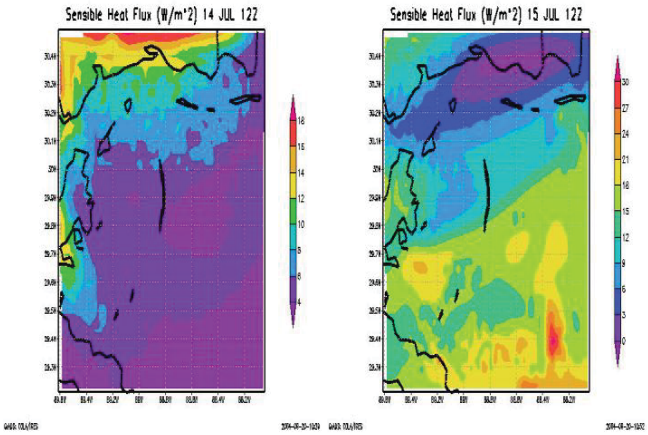

Figure 10. Sensible heat flux form MM5 output for July 14 and 15, 2004

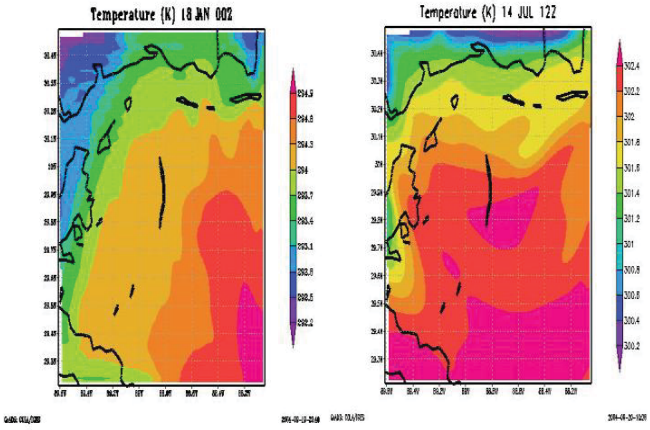

Figure 11. Surface temperature from MM5 output for January 18, and July 14, 2004

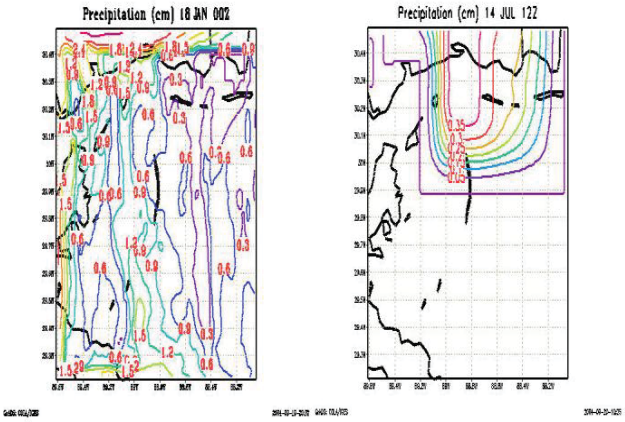

Figure 12. Precipitation from MM5 output for 18 January and July 14, 2004

CONCLUSIONS

Seasonal prediction for meteorological variables using environmental modeling MM5 have been studied for winter and summer seasons The sea level pressure is low during winter with an average of 1005 mb and high during the summer with an average of 1009 mb The heat fluxes are high during January with an average of 80 W/m^2 compared to July with an average of 30 W/m^2 The precipitation is maximum over the Grand Bay during January with a maximum of 1.85 cm compared to July with a maximum of 0.5 cm. Sea surface temperatures during the winter is low compared to summer over the Grand Bay region. The environmental model captured the seasonal variations and model output is in good agreement with observations.

Not many studies have been reported the modeling and observations of meteorological parameters and their impacts on habitants and ecosystem over Grand Bay. The model results and observations of climate and seasonal fluctuations over Grand Bay are clearly evinced warm temperatures during summer associated less precipitation and cold temperatures during winter associated with heavy precipitation. These may be due to land and sea breeze circulations and surface fluxes over the ocean. The impact assessment of ecosystem and fish population over the Grand Bay area will be further investigated.

ACKNOWLEDGEMENTS

The research is supported by the National Oceanic and Atmospheric Administration (NOAA) through the Environmental Cooperative Science Center, NOAA-ECSC Grant #NA17AE1626, Subcontract #27-0629-017 to Jackson State University.

LITERATURE CITED

Chigbu, P., Gordon, S., Strange, T.: 2004, Influence of inter-annual variations in climatic factors on fecal coliform levels in Mississippi Sound. *Water Research*.38 (20): 4341-4352.

Chigbu, P., Gordon, S.,Tchounwou, P.B.: 2005, Seasonal patterns of fecal coliform bacteria pollution and its influence on closures of shellfish harvesting areas in Mississippi Sound. International Journal of Environmental Research and Public Health, 2(2): 362-373.

Grell, G. A., J. Dudhia, and D. R. Stauffer, 2003, A description of the fifth-generation Penn State NCAR mesoscale Model (MM5), NCAR/ TN-398+STR, NCAR Technical Note, NCAR, Boulder, CO. 122pp.

Kain, J. S., and J. M. Fritsch.: 1993, The Representation of Cumulus Convection in Numerical Models, Meteor. Monger., No. 46, American Meteorological Society, 165-177pp.

Krishnamurti, T. N., Wei Han, Bhaskar. J., H. S. Bedi.: 1998, Numerical Prediction of Hurricane Opal. Monthly Weather

Opal. Monthly Weather Review**,** Vol. 126, No. 5, pp. 1347–1363.

Reddy, R. S., A. Schwartz, P. Remata, J. D. Sims.: 2003, A Study of Air-sea Interactions an Associated Tropical Cyclone/hurricane Activity over the Gulf of Mexico using Satellite Data and Numerical Modeling, Micro-Scale and Mesoscale air-sea interaction, Proc. of the 83rd American Meteorological Society Conference.

Reddy, R.S.: 2002, Mesoscale Modeling investigation of air-sea interactions over Gulf of Mexico for a case study of Hurricane Gordon, Proc., of Twelfth PSU/NCAR Mesoscale Model Users' Workshop, NAR, Boulder, CO, June 24 – 25, 2002.

Reddy, R.S., Williams, Q.L.: 2009, Variability of ocean-atmospheric interactions associated with tropical cyclone/hurricane Katrina. Proc. Of the 10th WRF Users' Workshop, NCAR, Boulder, Colorado, on 23-26 June

Reddy, R. S., D. Lu, Williams, Q.L.: 2009, A study of ocean-atmospheric interactions and associated tropical cyclone/hurricane activity over the Gulf of Mexico using Coupled Atmospheric Modeling System (CAMS), Proc., of the 16th AMS Conference on Air-Sea Interaction, Phoenix, AZ, 11-15 January 2009.

Remata, S.R, Varti,M.V, Chigbu, P.: 2003, Simulations of the southeast Louisiana and Southeastern Mississippi flood of May 8-10, 1995, with a Penn State/NCAR Mesoscale Model (MM5) and GIS RS Technology. **2003,** Proc. Of the 13th MM5 Users' Workshop, June 10 - 11, 2003, NCAR, Boulder, CO

Wang et al, W.: 2001, 'PSU/NCAR Mesoscale Modeling System Tutorial class Notes and User Guide: MM5 Modeling System URL:http://www.mmm.ucar.edu/mm5

White, L.D, Reddy, R.S.: 2001, Mesoscale Modeling Investigation of Air-sea Interactions over the Gulf of Mexico for a Case Study of Hurricane Bret, Proc., of the Symposium on precipitation, Impacts, and Responses, 14-18 January 2001, Albuquerque, New Mexico, American

82ND ANNUAL MEETING

THAD COCHRAN CONVENTION CENTER
HATTIESBURG, MS

FEBRUARY 22-23, 2019

SUBMIT ABSTRACTS BY
NOV. 15, 2018

Make sure to Renew Your Membership

Can also be done on-line at : http://msacad.org/

Membership/Registration opens December 1, 2017

Renew and join early to avoid late fees

83rd ANNUAL MEETING

THAD COCHRAN CONVENTION CENTER
HATTIESBURG, MS

FEBRUARY 21-22, 2019

SUBMIT ABSTRACTS BY
NOV. 15, 2018

Make sure to Register to receive Complimentary Membership

Can also be done on-line at : http://msacad.org/

Membership/Registration opens December 1, 2018

Renew and join early to avoid late fees

MISSISSIPPI ACADEMY OF SCIENCES ABSTRACT FORM/MEMBERSHIP FORM

ABSTRACT INFORMATION

Abstract Title:_____
Name of Presenting Author(s): _____
If you are a student please fill-out the next line
Name of Mentor and e-mail of Mentor _____
(Telephone_____Email_____

Check the division in which you are presenting

__ Agriculture and Plant Science
__ Biomaterials
___Cellular, Molecular, and Dev. Biol
__ Chemistry and Chem. Engineering
__ Ecology and Evolutionary Biology
__ Geology and Geography
__ Health Sciences/Population Health
__ History and Philosphy of Sciences
__ Math., Computer Sci and Statistics
__ Marine and Atmospheric Sciences
__ Physics and Engineering
__ Psychology and Social Sciences
__ Science Education
__ Zoology and Entomology

Complete either the Membership/Pre-Registration form if you plan to attend and present at the meeting if you do not plan to attend the meeting please complete the membership form

MEMBERSHIP/ PRE-REGISTRATION INFORMATION
New ___ Renewal___
Mr. Ms. Dr._____
Address _____
City, State, Zip _____
School or Firm _____
Telephone_____ **Email**_____

PLEASE INDICATE DIVISION YOU WISH TO BE AFFILIATED _____
Before January 8, 2019…….Regular Member/Pre-Registraion $130 Student Member/ Pre-registration $50
After January 8, 2019…….Regular Member/Registraion $180 Student Member/ Pre-registration $60

MEMBERSHIP INFORMATION
New ___ Renewal___
Mr. Ms. Dr._____
Address _____
City, State, Zip _____
School or Firm _____
Telephone_____ **Email**_____

PLEASE INDICATE DIVISION YOU WISH TO BE AFFILIATED _____
Regular Member $30 **Student Member $10** **Life Member $450**
Educational Member $550 **Corporate Patron $1000** **Corporate Donor $500**

CHECKLIST
Please complete the following:
__ Enclose title of abstract (even if abstract has been submitted electronically)
__ Complete membership/registration form (this form)
__ Enclose the following payments (Make checks payable to Mississippi Academy of Sciences)
__ $25 per abstract
__ $130 regular membership/pre-registration fee OR $50 student membership/pre-registration fee
__ You must supply a check #_____ or P.O. #_____ (or indicate Pay Pal confirmation) _____

MISSISSIPPI ACADEMY OF SCIENCES—ABSTRACT INSTRUCTIONS
PLEASE READ ALL INSTRUCTIONS BEFORE YOU SUBMIT YOUR ABSTRACT ON-LINE

- Your paper may be presented orally or as a poster. Oral presentations are generally 15 minutes. The speaker should limit the presentation to 10-12 minutes to allow time for discussion; longer presentations should be limited accordingly. Instructions for poster presentations are linked here.
- Enclose a personal check, money order, institutional check, or purchase order for $25 publication charge for each abstract to be published, payable to the Mississippi Academy of Sciences. The publication charge will be refunded if the abstract is not accepted.
- The presenting author must be a member of the Academy at the time the paper/poster is presented. Payment for membership of one author must be sent for the abstract to be accepted.
- Attendance and participation at all sessions requires payment of registration.
- Note that three separate fees are associated with submitting and presenting a paper at the annual meeting of the Mississippi Academy of Sciences.
    1. An abstract fee is assessed to defray the cost of publishing abstracts and
    2. A membership fee is assessed to defray the costs of running the Academy.
    3. Membership/Preregistration payment ($130 regular; $50 student) may accompany the abstract, or you may elect to pay this fee before January 8th, or pay full late membership/registration fees at the meeting ($180 regular, $60 student).
- Abstracts may **only** be submitted on line via a link through the MAS website.The appropriate abstract fees can be paid via Paypal or sent via mail to Barbara Holmes at the Academy address.
- **Late abstracts will be accepted with a $10 late fee during November increased to $25 after that. Late abstracts will be accepted only if there is room in the appropriate division. They will be published in the April issue of the MAS JOURNAL.**
- Submit your appropriate fees NO LATER THAN January 8h, 2019.

Ms. Lisa McCammon
Mississippi Academy of Sciences
Post Office Box 55907
Jackson, MS 39296-5907

GUIDELINES FOR POSTER PRESENTATIONS

- The Academy provides poster backboards. Each backboard is 36" high by 48"" wide. Mount the poster on the board assigned to you by your Division Chairperson. Please do not draw, write, or use adhesive material on the boards. You must provide your own thumb tacks.
- Lettering for your poster title should be at least 1" high and follow the format for your abstract. Lettering for your poster text should be at least 3/8" high.
- Posters should be on display during the entire day during which their divisional poster session is scheduled. They must be removed at the end of that day.
- Authors must be present with their poster to discuss their work at the time indicated in the program.

Author Guidelines

Editorial Policy. The Editorial Board publishes articles on all aspects of science that are of general interest to the scientific community. General articles include short reviews of general interest, reports of recent advances in a particular area of science, current events of interest to researchers and science educators, etc. Research papers of sufficiently broad scope to be of interest to most Academy members are also considered. Articles of particular interest in Mississippi are especially encouraged.

Research papers are reports of original research. Submission of a manuscript implies that the paper has not been published and is currently at the time of submission being considered for publication elsewhere. At least one of the authors must be a member of the Academy, and all authors are encouraged to join.

Manuscripts. Submit the manuscript electronically to the Mississippi Academy of Sciences under your profile in the member location of the website. Please also provide a cover letter to the Editor of the Journal. The cover letter should authorize publication: give the full names, contact information, for all authors; and indicate to whom the proofs and correspondence should be sent. Please notify the Editor on any changes prior to publication.

Manuscripts must adhere to the following format:

- One inch margins on 8.5 x 11 inch paper;
- Text should be left-justified using twelve point type;
- Double spaced throughout, including the title and abstract;
- Arabic numerals should be used in preference to words when the number designates anything that can be counted or measured (7 samples, 43 species) with 2 exceptions:
- To begin a sentence (Twenty-one species were found in…)
- When 2 numeric expressions are adjacent in a sentence. The number easiest to express in words should be spelled out and the other left in numeric form (The sections were divided into eight 4-acre plots.).
- Measurements and physical symbols or units shall follow the International System of Units (SI *Le Système international d'unités*) with metric units stated first, optionally followed by United States units in parentheses. *E.g.*: xx grams (xx ounces); and
- Avoid personal pronouns.

Format

Abstract. In 250 or fewer words summarize any new methods or procedures critical to the results of the study and state the results and conclusions.

Introduction. Describe the knowledge and literature that gave rise to the question examined by, or the hypothesis posed for the research.

Materials and methods. This section should describe the research design, the methods and materials used in the research (subjects, their selection, equipment, laboratory or field procedures), and how the findings were analyzed.

Results. The text of the results should be a descriptive narrative of the main findings, of the reported study. This section should not list tabulated data in text form. Reference to tables and figures included in this section should be made parenthetically in the text.

Discussion. In this section compare and contrast the data collected in the study with that previously reported in the literature. Unless there are specific reasons to combine the two, as explained by the author in the letter of transmittal, Results and Discussion should be two separate sections.

Acknowledgments. Colleagues and/or sources of financial support to whom thanks are due for assistance rendered in completion of the research or preparation of the manuscript should be recognized in this section rather than in the body of the text.

Literature cited. List references alphabetically. Cite references in the text by author and year of publication (e.g., Smith, 1975; Black and Benghuzzi, 2011; Smith et al., 2010; Smith, 2011a, 2011b). The following examples illustrate the style to be used in the literature list.

Black DA, Lindley S, Tucci M, Lawyer T, Benghuzzi H. A new model for the repair of the Achilles tendon in the rat. J Invest Surg. 2011; 24(5): 217-221.

Pearson HA, Sahukhal GS, **Elasri** MO, Urban MW. Phage-bacterium war on polymeric surfaces: can surface-anchored bacteriophages eliminate microbial infections? Biomacromolecules. 2013 May 13;14(5):1257-61.

Bold, H.C., C.J. Alexopoulos, and T. Delevoryas. 1980. Morpholgy of plants and fungi, 4th ed. Harper and Row, New York. 819 pp

Web-page

- name of author(s) -if known
- title of the work - in quotes, if known
- title of the Web page - in italics, if applicable
- date of last revision
- URL
- Date accessed

Example:

Ackermann, Ernest. "Writing Your Own Web Pages." *Creating Web Pages.* 23 Oct. 1996. http://people.umw.edu/~ernie/writeweb/writeweb.html 10 Feb. 1997.

File available by anonymous FTP

- name of author(s) -if known
- title of the work - in quotes, if known
- date of last revision
- URL
- Date accessed

Example:
American Civil Liberties Union. "Briefing paper Number 5, Drug Testing in the Work Place." 19 Nov. 1992. ftp://ftp.eff.org/pub/Privacy/Medical/aclu_drug_testing_workplace.faq 13 Feb. 1997.

Please Tables and Figures at the end of the manuscript submitted.

Tables. Tables must be typed double spaced, one table to a page, numbered consecutively, and placed at the end of the manuscript. Since tables must be individually typeset, consolidation of data into the smallest number of tables is encouraged. A horizontal double underline should be made beneath the title of the table, and single underlines should be made the width of the table below the column headings and at the bottom of the table. Do not use vertical lines, and do not place horizontal lines in the interior of the table. Use footnotes, to clarify possible questions within the table, should be noted by asterisks, daggers, or other symbols to avoid confusion with numerical data. Tables should be referred to parenthetically in the text, for example (Table 1).

Figures and illustrations. Figures may be photographs, computer -generated drawings, or graphs and should be placed at the end of the manuscript and referenced in the appropriate place.. All illustrations are referred to as “Figures” and must be numbered consecutively. Illustrations other than those generated by the author(s) must include permission for use and credit to the originator. Each figure must have a complete legend that is typed, double-spaced, on a separate sheet which precedes the figures in the manuscript. Figures should be referred to parenthetically in the text, for example (Fig. 1).

Footnotes. Text footnotes **should not be used**

Submission Preparation Checklist

As part of the submission process, authors are required to check off their submission's compliance with all of the following items, and submissions may be returned to authors that do not adhere to these guidelines.

1. The submission has not been previously published, nor is it before another journal for consideration (or an explanation has been provided in Comments to the Editor).
2. The text adheres to the stylistic and bibliographic requirements outlined in the Author Guidelines.
3. I acknowledge that if my manuscript is peer-reviewed and accepted for publication, there will be a paper charge fee of $50/page for **non-Academy members**.
4. The manuscript file is in Microsoft Word format.

Copyright Notice

Authors who publish with this journal agree to the following terms:

1. Authors retain copyright and grant the journal right of first publication
2. Authors are able to enter into separate, additional contractual arrangements for the non-exclusive distribution of the journal's published version of the work (e.g., post it to an institutional repository or publish it in a book), with an acknowledgement of its initial publication in this journal.
3. Authors are permitted and encouraged to post their work online (e.g., in institutional repositories or on their website) prior to and during the submission process, as it can lead to productive exchanges, as well as earlier and greater citation of published